

STEAM REFORMING OF METHANE IN A MEMBRANE REACTOR

A DISSERTATION

*Submitted in partial fulfillment of the
requirements for the award of the degree*

of

MASTER OF TECHNOLOGY

in

CHEMICAL ENGINEERING

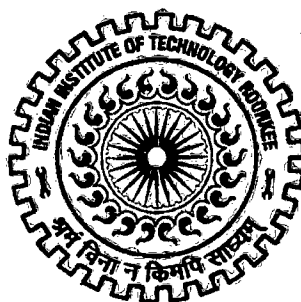
(with specialization in Computer Aided Process Plant Design)

By

ELAGONDA RAMAKRISHNA



613250



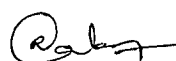
**DEPARTMENT OF CHEMICAL ENGINEERING
INDIAN INSTITUTE OF TECHNOLOGY ROORKEE
ROORKEE - 247 667 (INDIA)
JUNE, 2007**

CANDIDATE'S DECLARATION

I hereby declare that the work, which is being presented in this thesis report, entitled “**STEAM REFORMING OF METHANE IN A MEMBRANE REACTOR**”, submitted in partial fulfillment of the requirements for award of the degree of **Master of Technology in Chemical Engineering** with the specialization in **Computer Aided Process Plant Design (CAPPD)**, is an authentic record of my own work carried out under the supervision of **Dr. Surendra Kumar**, Professor and **Dr. Shishir Sinha** Assistant Professor, Department of Chemical Engineering, Indian Institute of Technology Roorkee.

Date: 25/06/07,

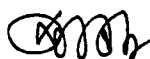
Place: Roorkee



(ELAGONDA RAMAKRISHNA)

.....

This is to certify that the above statement made by the candidate is correct to the best of my knowledge.



Dr. Surendra Kumar,

Professor,

Dept of Chem. Engg,

I.I.T Roorkee

Uttarakhand-247667,

INDIA.



Dr. Shishir Sinha

Assistant Professor,

Dept of Chem. Engg,

I.I.T Roorkee

Uttarakhand-247667,

INDIA.

Acknowledgement

I feel great pleasure in expressing my deep sense of gratitude to my guide **Dr. SURENDRA KUMAR**, Professor, Department of Chemical Engineering, Indian Institute of Technology Roorkee, for his valuable guidance, keen cooperation, useful criticism and self confidence which has contributed much in this work and my personal encouragement.

I would also like to thank my co-guide **Dr. Shishir Sinha**, Assistant Professor, Department of Chemical Engineering, Indian Institute of Technology Roorkee, for his encouragement, and help during all phases of the present study.

I would like to thank **Dr. (Mrs.) Shashi** for her cooperation in various stages of my work

I would like to thank to **Dr. Shri Chand**, Professor, D.R.C Chairman and Head, Department of Chemical Engineering, Indian Institute of Technology Roorkee for providing me with best of facilities during my work.

I would like to thank to, Mallareddy K, Sekhar babu, Upendar, Ramesh and Nitin and to all of my classmates for their suggestions and help in completion of the dissertation work.

I would like to thank Tripta didi, Z.Rahman Ji, Mangee Ram Ji, and all CAD lab members for their kind cooperation.

Last but not the least, it is allowed to the blessings of my parents and God that I have come up with this work in due time.

Thanks are due to Institute Computer Centre and Department CAD centre facilities.


ELAGONDA RAMAKRISHNA

ABSTRACT

In today's scenario of pollution world there is a need to produce fuels which do less pollution like Hydrogen. Methane reforming in membrane reactor is one of the processes to produce ultra pure hydrogen (99.999%). Today it is one of the fields in which many researchers are paying attention to. In my present work, model equations for Steam reforming of methane in a Pd/SS membrane reactor based on axial dispersion model and PFR assumptions are developed. Model equations are developed for key components and solved them through MATLAB 7. Various parameters affecting the conversions of CH_4 , CO_2 , and permeation of H_2 are calculated for a wide range of their availability. After the study it is always recommended that care has to be taken while designing process strategy as temperature and steam to methane ratio are affecting greatly the conversion. And it is also recommended to conduct this Reaction Scheme in a membrane reactor which can perform close to Ideal reactor model.

CONTENTS

CANDIDATE'S DECLARATION	i
ACKNOWLEDGEMENT	ii
ABSTRACT	iii
CONTENTS	iv
NOMENCLATURE	vi
LIST OF GRAPHS AND FIGURES	ix
LIST OF TABLES	x
1. CHAPTER 1	01
1.1 Introduction	01
1.2 Membrane reactor	02
1.3 Catalytic membrane reactor	04
1.4 Methane steam reforming	06
1.5 Methane reforming in catalytic membrane reactor	08
1.6 Literature review	10
1.7 Objective of the thesis	13
2. CHAPTER 2	14
2.1 Kinetics of reactions	14
2.2 Governing model equations	16
3. CHAPTER 3	22
Results and discussion	22
3.1 Effect of Temperature	23
3.2 Effect of Reaction zone pressure	25

3.3	Effect of reactants flow rate	28
3.4	Effect of steam to methane ratio	31
3.5	Effect of sweep factor	34
3.6	Effect of Catalyst weight	37
3.7	Effect of Membrane thickness	39
3.8	Effect of reactor length	42
4.	CONCLUSIONS	45
5.	BIBLIOGRAPHY	46
Appendix		
1.	MATLAB Model to solve PFR model equations	48
2.	MATLAB Model to solve axial dispersion model equations	51

NOMENCLATURE:

D: dispersion coefficient

D_i, D_0 : Inner, outer diameters of the reactor shell,

E_p : activation energy of permeation (kJ/mol)

$F_{CH_4}^0$: Initial feed molar flow rate

$F_{H_2}^{p, outlet}$: Molar flow rate of H_2 coming from permeation zone

$\Delta H_{298 K}$: the heat of reaction at 298 K

$J_{H_2}^{Permeating}$: Permeation flux of H_2 for membrane

K_1 : equilibrium constant 1

K_2 : equilibrium constant 2

K_3 equilibrium constant 3

$K_4 = K_{CH_4}$: CH_4 Adsorption constant

$K_5 = K_{H_2O}$: H_2O dissociative adsorption constant

$K_6 = K_{H_2}$: H_2 Adsorption constant

$K_7 = K_{CO}$: CO Adsorption constant

L: reactor length,

m : steam-to-methane ratio

PSA: Pressure swing absorption

P_{H_2} : Partial pressure of hydrogen

$P_{H_2}^0$: Initial partial pressure of hydrogen

P_{CO_2} : Partial pressure of CO₂

P_{CO} : Partial pressure of CO

P_{H_2O} : Partial pressure of H₂O.

P_{CH_4} : Partial pressure of CH₄.

$P_{H_2,r}$, $P_{H_2,p}$: The partial pressures of hydrogen on the reaction and permeation side of the membrane.

Q_0 : pre exponential factor of hydrogen permeation

R_1 : Rate of reaction 1

R_2 : Rate of reaction 2

R_3 : Rate of reaction 3

R_{CH_4} : Rate of decomposition of CH₄

R_{H_2O} : Rate of decomposition of CH₄

R_{CO} : Rate of formation of CO

R_{CO_2} : Rate of formation of CO₂

R_{H_2} : Rate of formation of H₂

u : average velocity of reaction mixture.

V^r : volume of reaction zone. $V^r = \pi (D_0^2 - D_i^2) L / 4$

Wt : weight of the catalyst.

x_{CH_4} : Total conversion of CH_4

x_{CO_2} : CH_4 conversion to CO_2

y_H : Permeation of H_2

Greek letters:

ρ_C : catalyst density = (approximately) Wt/V^r

σ : Parameter used while calculation

δ : Membrane thickness

List of Graphs and figures

S.No.	Description	Page
1.	Line diagram of membrane reactor in which catalyst packed in the annulus	05
2.	Line diagram of membrane reactor in which catalyst packed in the core of tube	05
3.	(a) Scheme of membrane reactor,	09
	(b) Detailed scheme of membrane reactor	09
4.	Mechanism of methane steam reforming reactions	14
5.	Effect of temperature on conversions of CH ₄ and CO ₂ in plug flow model	23
6.	Effect of temperature on Permeation of H ₂ in plug flow model	23
7.	Comparison of temperature effect on conversions of CH ₄ in dispersive flow model	24
8.	Comparison of temperature effect on conversions of CO ₂ in dispersive flow model	24
9.	Pressure effect on conversions of CH ₄ , CO ₂ in plug flow model at 773 K	26
10.	Effect of pressure on Permeation of H ₂ in plug flow model at 773 K	27
11.	Comparison of pressure effect on conversion of CH ₄ in dispersive flow model at 773 K	27
12.	Comparison of pressure effect on conversion of CO ₂ in dispersive flow model at 773 K	28
13.	Effect of reactants flow rate on conversions of CH ₄ , CO ₂ in plug flow model at 773 K	29
14.	Effect of reactants flow rate on Permeation of H ₂ in plug flow model at 773 K	29
15.	Comparison of reactants flow rate effect on conversion of CH ₄ in dispersive flow model at 773 K	30
16.	Comparison of reactants flow rate effect on conversion of CO ₂ in dispersive flow model at 773 K	30
17.	Effect of steam to methane ratio on conversions of CH ₄ , CO ₂ in plug flow model at 773 K	32
18.	Effect of steam to methane ratio on Permeation of H ₂ in plug flow model at 773 K	32
19.	Comparison of steam to methane ratio on conversions of CH ₄ in dispersive flow model at 773 K	33

20. Comparison of steam to methane ratio on conversions of CO ₂ in dispersive flow model at 773 K	33
21. sweep factor effect on conversions of CH ₄ , CO ₂ in plug flow model at 773 K	35
22. Effect of sweep factor on Permeation of H ₂ in plug flow model at 773 K	35
23. Comparison of sweep factor on conversions of CH ₄ in dispersive flow model at 773 K	36
24. Comparison of sweep factor on conversions of CO ₂ in dispersive flow model at 773 K	36
25. Effect of catalytic weight on conversions of CH ₄ , CO ₂ in plug flow model at 773 K	37
26. Effect of catalytic weight on Permeation of H ₂ in plug flow model at 773 K	38
27. Comparison of catalytic weight on conversions of CH ₄ in dispersive flow model at 773 K	38
28. Comparison of catalytic weight on conversions of CO ₂ in dispersive flow model at 773 K	39
29. Effect of membrane thickness increment on conversions of CH ₄ , CO ₂ in plug flow model at 773 K	40
30. Effect of membrane increment thickness on Permeation of H ₂ in plug flow model at 773 K	41
31. Comparison of membrane thickness increment on conversions of CH ₄ in dispersive flow model at 773 K	41
32. Comparison of membrane thickness increment on conversions of CO ₂ in dispersive flow model at 773 K	42
33. Comparison of reactor length effect on conversions of CH ₄ and CO ₂ at 773 K	43
34. Comparison of reactor length effect on Permeation of H ₂ in plug flow model at 773 K	43
35. Effect of reactor length on conversion of CH ₄ in dispersive flow model at 773 K	44
36. Effect of reactor length on conversion of CO ₂ in dispersive flow model at 773 K	44

LIST OF TABLES

1. Distribution of components in Syngas	02
2. Kinetics parameters of methane steam reforming	18
3. Reactor specifications	18

1.1 Introduction

Synthesis gas or syngas is a mixture of hydrogen and carbon monoxide used as a major intermediary for the production of pure hydrogen or other chemical compounds. Among these we have to mention ammonia with its inestimable utility for industry and agriculture and the liquid products derived by the process known as syngas conversion to liquids (e.g. methanol and other alcohols, solvents, diesel fuel, jet fuel, gasoline, etc). The growing demand for chemicals derived from syngas has led to the development of several technologies (e.g. Fischer–Tropsch synthesis, NH_3 or oxygenate production). These processes are of strategic importance for any country. For example, the synthesis developed by Fischer and Tropsch was used by the Germans during the Second World War to produce fuel from coal. Methane steam reforming consists in the reaction of CH_4 and steam on a supported Ni catalyst to produce a mixture of H_2 , CO , CO_2 and CH_4 . This technology has been proved more economic than other processes such as coal vaporization, hydrocarbon partial oxidation, water electrolysis to produce hydrogen for the reduction of iron ores, for the use in fuel cells and for hydro cracking, etc. Currently, this process is the main route to obtain hydrogen and synthesis gas for ammonia and methanol. Today, as the fuels obtained from syngas do not contain sulphur or nitrogen compounds, their combustion in engines leads to reduced environmental pollution. Hydrogen itself was taken into account in the last period as a clean fuel, important steps being made in the research in recent years on the on board production of hydrogen for automotive applications. Syngas is also the main source of carbon monoxide, which is used in an expanding list of carbonylation reactions. Originally, coal was the primary source of carbon for syngas, but today natural gas has replaced it for economic reasons. Despite the fact that coal reserves are large and the price of coal is lower than that of the hydrocarbons, the investment in a coal based syngas plant is about three times higher than that required for a natural gas based plant. However, there are also technologies producing syngas from petroleum coke, heavy residuals and even biomasses.

Natural gas can be processed by several methods, e.g. partial oxidation with oxygen, steam reforming, and steam reforming with oxygen, CO_2 reforming and CO_2 reforming with oxygen. One of the most attractive technologies seems to be the steam reforming. The syngas composition of processes with water coal slurry systems is (vol %)

Table 1: Distribution of components in Syngas

Component	Volume percentage
CO	35-45
CO ₂	10-15
H ₂	27-30
H ₂ O	15-25
H ₂ S	0.2 - 1.2
HCl	50-500 ppm

For a dry fed gasifier the CO content of the gas is considerably higher 62-64%, while the CO₂ and H₂O contents are generally less than 4%. Syngas has a heating value of 125 - 350 BTU/s.cf.

Methane steam reforming in industry is carried out in a catalytic multi tubular fixed bed reactor. The reforming plant is composed of two units the primary reformer, where the methane and water steam reaction occurs and the secondary reformer, where air is added to supply both the nitrogen necessary for ammonia synthesis and the oxygen to react with the non converted methane to produce carbon monoxide and hydrogen.

Methane steam reforming involves two reversible reactions reforming and the water gas shift reaction. The first is endothermic and limited by thermodynamic equilibrium. Therefore, the development of a membrane based separation process can open up the possibility of increasing the conversion of the reforming process. As hydrogen is selectively removed from the reactor, the chemical equilibrium of the reactions is shifted to the product, resulting in an increase in the conversion of methane to hydrogen and carbon dioxide. As an additional advantage, the membrane reactor offers the possibility of supplying hydrogen with the same conversion degree but higher purity, than that supplied by the conventional reactor, under less severe operational conditions. Methane steam reforming in a membrane reactor is not an equilibrium limited reaction, but rather a mass transfer limited reaction related with membrane porosity and diffusivity.

1.2 Membrane reactor

Membrane reactor is a new reaction system where membranes and chemical reaction are combined together. A membrane reactor is really just a plug flow reactor that contains an

additional cylinder of some porous material within it, kind of like the tube within the shell of a shell-and-tube heat exchanger. This porous inner cylinder is the membrane that gives the membrane reactor its name. The membrane is a barrier that only allows certain components to pass through it. The selectivity of the membrane is controlled by its pore diameter, which can be on the order of angstroms, for micro porous layers, or on the order of micro meters for macro porous layers. The membrane reactors have a number of different types of reactor configurations containing membranes inside. The membrane can provide a barrier to a number of components of the reaction effluents, while permitting permeation by others, or it may be used as a catalyst support by depositing a catalytically active component on it. The membrane reactor has been used to increase conversions in thermodynamically or kinetically-limited catalytic processes. This reactor is applied to obtain conversion levels up to the theoretical equilibrium value. These higher conversion levels can be obtained as a consequence of the shift in thermodynamic equilibrium of the reversible reactions in the direction of product formation, as a consequence of removal by a diffusion mechanism of a product desirable for the semi permeable membrane. Based on this concept, incorporation in reactors of a separation membrane, especially a selective membrane for hydrogen separation, has been proposed and studied (E.M. Assaf et al, 1992, Uemiya et al., 1991, Kikuchi et al., 1991, Deng and wu, 1994, Chai et al., 1994).

Membrane reactors combine reaction with separation to increase conversion. One of the products of a given reaction is removed from the reactor through the membrane, forcing the equilibrium of the reaction "to the right" (Le chatelier's principle), so that more of that product is produced. Membrane reactors are most commonly used when a reaction involves some form of catalyst, and there are two main types of these membrane reactors

1. Inert membrane reactor
2. Catalytic membrane reactor

The inert membrane reactor allows catalyst pellets to flow with the reactants on the feed side (usually the inside of the membrane). It is known as an IMRCF, inert membrane reactor with catalyst on the feed side. In this kind of membrane reactor, the membrane does not participate in the reaction directly; it simply acts as a barrier to the reactants and some products.

A catalytic membrane reactor has a membrane that has either been coated with or is made of a material that contains catalyst, which means that the membrane itself participates in the

reaction. Some of the reaction products (those that are small enough) pass through the membrane and exit the reactor on the permeate side.

Membrane reactors are commonly used in dehydrogenation reactions (e.g., dehydrogenation of ethane), where only one of the products (molecular hydrogen) is small enough to pass through the membrane. This raises the conversion for the reaction, making the process more economical.

Membrane reactors with packed bed catalyst have separation zone separated from reaction zone. On the other hand, in catalytic membrane reactors, reaction and separation occurs simultaneously.

The membrane reactor has two individual compartments separated by a chemically specific membrane. Each compartment can hold a different solution, for instance one can contain the catalyst and the other the starting materials/products. Additionally the membrane itself can contain an immobilized catalyst and the two compartments can hold the reagents and products separately. It can provide benefits in separating products, reagents or catalysts, which can eliminate the need for solvent intensive workup procedures.

1.3 Catalytic membrane reactor

The catalytic membrane reactor consists of two concentric pipes the inner one is the membrane, whereas the outer is a stain less steel shell. The sealing between these two parts is realized by means of graphite o rings. The catalyst can be packed in the annular space or in the core of the tube. When the catalyst is packed in the annulus the reactor will named annular membrane reactor; in other case, the reactor will be indicated as tubular membrane reactor. In the other side, the sweep gas flows in co current or counter current flow mode with the reactant stream. Both retentate and permeate streams are analyzed by means of a gas chromatograph.

Most of the membranes are made up of very thin dense film of metal or alloys deposited on a tubular support of ceramic materials, with the following different techniques (Giuseppe, 1997)

1. Electro less plating
2. Solvated metal atom deposition
3. Chemical vapor deposition
4. Sputtering

The first technique allows the deposition of the metallic film on the external surface of the support. With the second one the deposition can be carried out also on the inner surface of the tubular support.

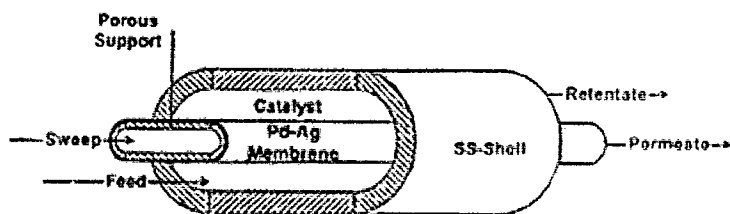


Fig 1: Catalyst packed in the annulus (Giuseppe marigliano 2001)

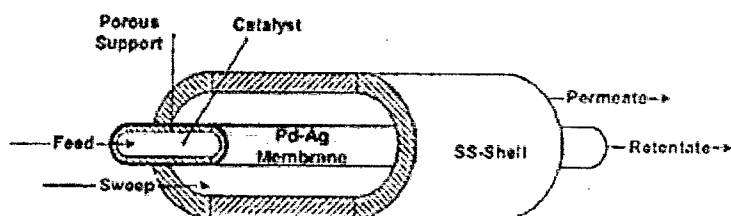


Fig 2: Catalyst packed in the core of tube (Giuseppe marigliano 2001)

Above figure shows the two conventional methods of operation of a particular type of membrane reactor. Depending on the situation one could select any one of them. For our purpose the first type, catalyst packed on shell side was used. The reason is only the convenience of supplying heat from out side. Inorganic membrane reactors are considered to be multifunctional reactors because they are able to combine catalytic reactions with membrane separation properties. In particular, dense palladium membranes are characterized by the following facts.

1. Only hydrogen might permeate through them
2. Both Arrhenius and sievert laws are followed.

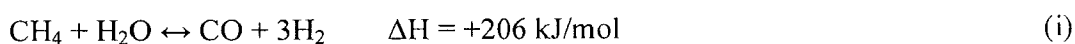
The drawback in using palladium membranes in large scale reforming plants is the availability and the price of palladium metal. Furthermore the hydrogen permeability of conventional palladium (alloy) membranes is low compared to the very high catalytic reaction rates and the high industrial space velocities. The development of membrane reactors with high permeation rates is desirable. The only way to drastically increase the permeation rate is to decrease the membrane thickness.

1.4 Methane steam reforming

Process description

Catalytic steam reforming of methane is a well known, commercially available process for hydrogen production. Hydrogen production is accomplished in several steps

1. Steam reforming
2. Water gas shift reaction
3. Hydrogen purification



The steam reforming reaction is endothermic and requires external heat input. Economics favor reactor operation at pressures of 3-25 atmospheres and temperatures of 700°C to 850°C. The external heat needed to drive the reaction is often provided by the combustion of a fraction of the incoming natural gas feedstock (up to 25%) or from burning waste gases, such as purge gas from the hydrogen purification system. Heat transfer to the reactants is accomplished indirectly through a heat exchanger. Methane and steam react in catalyst filled tubes. Typically, the mass ratio of steam to carbon is about 3 or more to avoid "coking" or carbon build up on the catalysts. (At lower steam-to-carbon ratios, solid carbon can be produced via side reactions.)

After reforming, the resulting syngas is sent to one or more shift reactors, where the hydrogen output is increased via the water gas shift reaction.



Water gas shift reaction converts CO to H₂, this reaction is favored at temperatures of less than 600°C, and can take place as low as 200°C, with sufficiently active catalysts. The gas exiting the shift reactor contains mostly H₂ (70%-80%) plus CO₂, CH₄, H₂O and small quantities of

CO. For hydrogen production, the shift reaction is often accomplished in two stages. A high temperature shift reactor operating at about 350-475°C accomplishes much of the conversion, followed by a lower temperature (200-250°C) shift reactor, which brings the CO concentration down to a few percent by volume or less. Hydrogen is then purified. The degree of purification depends on the application. For industrial hydrogen, pressure swing absorption (PSA) systems or palladium membranes are used to produce hydrogen at up to 99.999% purity. For proton exchange membrane (PEM) or phosphoric acid fuel cells closely coupled to reformers, diluents such as CO₂ and CH₄ are tolerable. However, CO must be reduced to less than about 10 ppm for PEM fuel cells, so a CO removal system such as preferential oxidation must be used. In a preferential oxidation system, the gas is passed over a catalyst bed, with added air. At certain temperature and stoichiometric conditions,



This reaction is strongly favored over hydrogen oxidation, so that CO is removed to the level of several ppm. Preferential oxidation technology is being developed for use with reformers in fuel cell cogeneration systems or onboard fuel cell vehicles. The energy conversion efficiency [= hydrogen out (higher heating value (HHV))/energy input (HHV)] of large scale steam methane reformers is 75%-80%, although 85% efficiencies might be achieved with good waste heat recovery and utilization.

The main reactions in the steam reforming process are the hydrocarbon to carbon monoxide conversion (reformation of natural gas) and the water gas shift (Xu, J et al 1989).

1. $\text{CH}_4 + \text{H}_2\text{O} \leftrightarrow \text{CO} + 3\text{H}_2$ $\Delta H_{298\text{K}} = 206 \text{ kJ/mol}$
2. $\text{CO} + \text{H}_2\text{O} \leftrightarrow \text{CO}_2 + \text{H}_2$ $\Delta H_{298\text{K}} = -41 \text{ kJ/mol}$
3. $\text{CH}_4 + 2\text{H}_2\text{O} \leftrightarrow \text{CO}_2 + 4\text{H}_2$ $\Delta H_{298\text{K}} = 165 \text{ kJ/mol}$

Other possible reactions:

4. Methane cracking $\text{CH}_4 \leftrightarrow \text{C} + 2\text{H}_2$ $\Delta H_{298\text{K}} = 75 \text{ kJ/mol}$
5. Boudouard reaction: $2\text{CO} \leftrightarrow \text{C} + \text{CO}_2$ $\Delta H_{298\text{K}} = -173 \text{ kJ/mol}$
6. Total combustion of CH₄: $\text{CH}_4 + 2\text{O}_2 \leftrightarrow \text{CO}_2 + 2\text{H}_2\text{O}$
7. Dry reforming of methane: $\text{CH}_4 + \text{CO}_2 \leftrightarrow 2\text{CO} + 2\text{H}_2$ $\Delta H_{298\text{K}} = 247 \text{ kJ/mol}$
8. Carbon gasification by steam: $\text{C} + \text{H}_2\text{O} \leftrightarrow \text{CO} + \text{H}_2$ $\Delta H_{298\text{K}} = -131 \text{ kJ/mol}$
9. Carbon gasification by O₂: $\text{C} + \text{O}_2 \leftrightarrow \text{CO}_2$

Various types of steam methane reformers

1. Conventional steam methane reformers
2. Compact “fuel cell type” steam methane reformers with concentric annular catalyst beds
3. Plate type steam methane reformers
4. Membrane reactors for steam reforming

1.5 Methane steam reforming in membrane reactor

Methane reforming in membrane reactors is a technology, where the steam reforming, water gas shift and hydrogen purification steps all take place in a single reactor. The hydrogen separation membranes used in these membrane reactors are of two kinds (Uemiya 1991):

1. Porous Vycor glass
2. Palladium or its alloys

The limitation on the attainable level of conversion forms a disadvantage of the membrane reactor using porous Vycor glass membrane, in which gas separation is based on the Knudsen diffusion. On the other hand, the palladium membrane reactor can attain high levels of conversion (even 100%), the drawback here being its low efficiency or low rate of reaction.

In methane steam reforming, the catalytic fixed bed reactor is fed with a gas mixture of CH_4 and H_2O in a molar ratio from 1:3 to 1:4. The commercial catalyst is composed of Nickel supported on γ -Alumina. The industrial reactor is composed of vertical tubes (between 10 and 900) with internal diameters from 7 to 16 cm and lengths from 6 to 12 m, inserted in to a radiant furnace chamber (Shu et al 1994). The entrance reactor temperature is 600°C and pressures vary from 1 to 4.0 MPa. Such a high range pressures are used to improve the energy efficiency of the process. 78% conversion of methane at temperatures up to 850°C is commonly achieved with above feed ratios (E.M.Assaf et al 1999). Exit temperature is limited by the metallurgical limitations of the tubes, since at higher temperatures the metal tube may creep under stress.

High temperatures favor the process due to the endothermic nature of the reaction. These conditions are quite strenuous as regards construction material and, therefore, expensive steel alloys are used. From this point of view, there will be a considerable incitement to lower the reaction temperature. The equilibrium limitation is to be overcome for above purpose.

Therefore, the reaction should be carried out either at a very low pressure or in a membrane reactor (selective removal of one component). If hydrogen is selectively removed from the reaction system, high reaction temperatures are not necessarily required from thermodynamic viewpoint. In addition, if membrane is permeable only to hydrogen like palladium, fuel hydrogen containing little carbon monoxide can be produced without further purification.

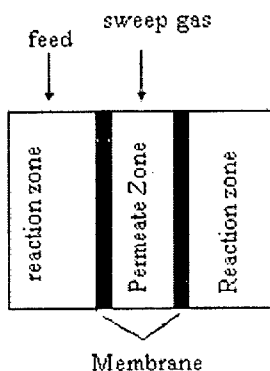


Fig 3(a): Scheme of membrane reactor (Fabiano A.N et al, 2006)

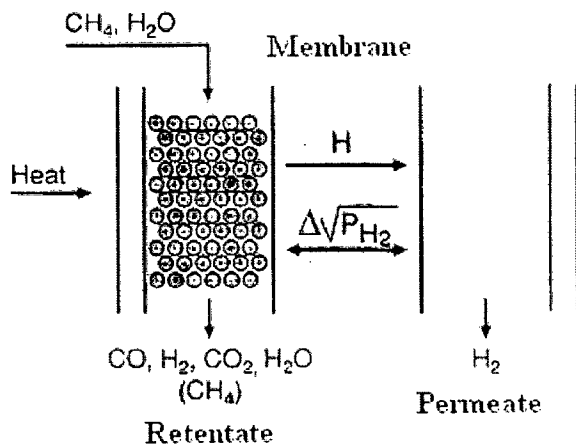


Fig 3(b): Detailed diagram of membrane reactor

The steam reforming plant based on the membrane reactor seems simpler than the traditional reactor because

1. Successive purification steps based on the CO shift reaction
2. Pressure Swing Absorption (PSA) are not required anymore to produce pure H₂

The membrane steam reformer reactor can work at lower temperatures. The H₂ produced does not contain CO but only H₂O, depending on the efficiency of the final condensation step. But still there are some practical obstacles to the real application of the membrane steam reforming process.

1. First of all, the membrane reformer technology has to compete with the traditional technology that is well established and optimized. In this view, the first membrane steam reformer installation could be expensive because the entire process plant has to be reconsidered for the optimization of the successive plants.
2. Then the Pd cost is quite high, and the reactor has to be optimized in order to have the highest H₂ production efficiency with the lowest amount of membrane. Alternatively, others materials with both high H₂ permeability and lifetime have to be considered for the membrane.

In this work we show the suitability of the palladium membrane reactor for the steam reforming of methane and describe the dependence of methane conversion on the reaction conditions, which exert a great influence on hydrogen permeation, especially the flow rate of sweep gas and the reaction Temperature.

1.6 Literature review:

Jiang uo Xu Gilbert F. Froment et al (1989): Intrinsic rate equations were derived for the steam reforming of methane, accompanied by water-gas shift on a Ni/MgAl₂O₄ catalyst. A large number of detailed reaction mechanisms were considered. Thermodynamic analysis was used to reduce the number of possible mechanisms. Twenty one sets of three rate equations were retained and subjected to model discrimination and parameter estimation. The parameter estimates in the best model, are statistically significant and thermodynamically consistent. These kinetic expressions are used for present study.

Uemiya (1991): Steam reforming of methane was carried out in a reactor incorporating a hydrogen-permeable membrane, which consisted of a thin palladium film supported on a porous glass cylinder. Comparison of 2 membranes porous Vycor glass membrane and palladium membrane was carried out through experimental work. It was shown that the supported palladium membrane promoted the hydrogen production reaction more effectively than a porous Vycor glass membrane. The level of methane conversion exceeded the

equilibrium attainable in a closed system in the temperature range of 623-773 K as a result of selective removal of hydrogen from the reaction system. Under the same conditions the porous Vycor glass membrane exhibited little effect on the shift of equilibrium. The difference between these two types of membranes is attributed to their hydrogen permeabilities. Although high reaction pressures are thermodynamically unfavorable for steam reforming, the level of methane conversion in the palladium membrane reactor increased with increasing pressure on the reaction side, as a result of accelerated hydrogen flow to the permeation side.

Shu et al (1994): Their work is devoted to applying electrolessly deposited Pd and Pd - Ag/porous stainless steel composite membranes in methane steam reforming. The methane conversion was significantly enhanced by the partial removal of hydrogen from the reaction location as a result of diffusion through the Pd based membranes. For example, at a total pressure of 136 kPa, a temperature of 500 °C, a molar steam to methane ratio of 3, and in the presence of a commercial Ni/Al₂O₃ catalyst together with continuous pumping on the permeation side, a methane conversion twice as high as that in a non-membrane reactor was reached by using a Pd/SS membrane. In this work comparison of Pd/SS, Pd-Ag/SS membranes with that of non membrane system are carried out through experimental work. The effects of some independent parameters were examined under a variety of experimental conditions. A computer model of the membrane reactor on the basis of PFR assumptions and infinite permselectivity to hydrogen was also developed to predict the effects of membrane separation on methane conversion. For my present work the results from this paper is used as reference.

S.Lægsgaard (1995): Methane reforming in a Pd/Ag membrane reactor was carried out. Conversion of CH₄ with Temperature for wide range of operation is carried out. A new parameter called H/C ratio is defined in the following way.

$$H / C = \frac{2Y_{H_2} + 2Y_{H_2O} + 4Y_{CH_4}}{Y_{CH_4} + Y_{CO} + Y_{CO_2}}$$

Y_i = mole fraction of component “i” in the exit gas stream.

Carbon free operation is carried out successfully in the experimental work and a criterion for it (H/C ratio ≥ 6) is established. The operational limits for the steam-to-methane ratio are discussed. To avoid carbon formation, this ratio has to be higher in a Pd/Ag membrane reactor than in a conventional steam reforming tubular reactor.

Giuseppe Barbieri (1997) Simulation of reactors with parallel-flow and counter flow configuration had been performed to study the methane steam reforming reaction in a packed-bed inert membrane reactor (PBIMR). In this kind of reactor complete methane conversion can be achieved by means of the total removal of hydrogen from the reaction products. In the model on basis of PFR assumptions and infinite permselectivity to hydrogen, a dense Pd membrane was simulated. Membrane reactor performance was compared to that of a conventional fixed-bed reactor. The effect on the degree of conversion was analyzed for different parameters such as temperature, reactor pressure, feed and sweep flow rate, feed molar ratio, membrane thickness, and space velocity. Comparison with experimental data of Shu et al. (1994) showed a good agreement. An analysis of the results indicated that the choice of operating conditions requires a complex process strategy.

Giuseppe Barbieri (2001): An analysis of the conversion temperature diagram for methane steam reforming was presented. A mathematical model of a membrane reactor containing a Pd-based membrane with ideal behavior (PFR) was developed to calculate the temperature and species profiles. The comparison of annular and tubular configurations showed different membrane reactor performance because of thermal effects. The equilibrium of the membrane reactor system was calculated, starting from the method of “reactors in series”. The equilibrium curve of a membrane reactor was calculated as a function of the sweep factor (I), defined as the ratio of the sweep gas and methane feed flow rates. The existence region for a membrane reactor was defined as a function of “ I ” and is delimited by the adiabatic, isothermal, and equilibrium curves. Once I , the feed molar ratio, and the oven temperature were defined, the reaction paths of all membrane reactors fall within the existence region. This was observed for various values of reaction rates, membrane thicknesses, flow rates, overall heat transfer coefficients, and geometric parameters. The existence region of a membrane reactor was, therefore, an extension of that in a traditional reactor, achieving better performance with increased methane conversion.

A. Bottino (2006): This paper presents the model of a non adiabatic methane steam reformer membrane reactor (MSRMR) working in equilibrium conditions.

1. MSRMR is assumed to be a train of single isothermal stages where the equilibrium composition is established in a reaction chamber at the stage temperature.
2. In the reaction chambers it is assumed that the equilibrium composition will take place. This fact states that the phenomenon which keeps a system out of equilibrium

conditions is not taken into consideration (fluid dynamic, heat and mass transfer limitations). In each single part of the MSRMR perfect mixing is assumed.

3. In order to study the MSRMR performance a membrane with similar characteristics to those of a Pd membrane are considered.

The model was used to investigate the effects of some variables (e.g. temperature profile, separation efficiency, plant size) on the membrane area and the energy required by the process, which in turn affect fixed and operating costs. The simulations showed that the membrane area required sharp increases in the reactor size and that for large plants the development of thin and permeable membranes is a key issue.

Fabiano A.N (2006): A mathematical model of a membrane reactor used for methane steam reforming was developed on basis of PFR assumptions to simulate and compare the maximum yields and operating conditions in the reactor with that in a conventional fixed bed reactor. Results show that the membrane reactor resents higher methane conversion yield and can be operated under milder conditions than the fixed bed reactor, and that membrane thickness was the most important construction parameter for membrane reactor success. Control of the H_2/CO ratio was possible in the membrane reactor making this technology more suitable for production of syngas to be used in gas-to-liquid processes (GTL).

1.7 Objective of the thesis:

In this work, the model equations of steam reforming of methane in membrane reactor introducing a new term called “Dispersion coefficient” are developed. Hence the model equations become non ideal in nature and predicting the effect of dispersive coefficient on all possible parameters is the main objective of this work.

2.1 Kinetics:

The kinetic model for the reaction on a Ni/MgAl₂O₄ catalyst is based on a Longmuir - Hinshelwood reaction mechanism which involves 13 steps and the rate expressions for above reactions (1 to 3) are given by Xu J, et al (1989)

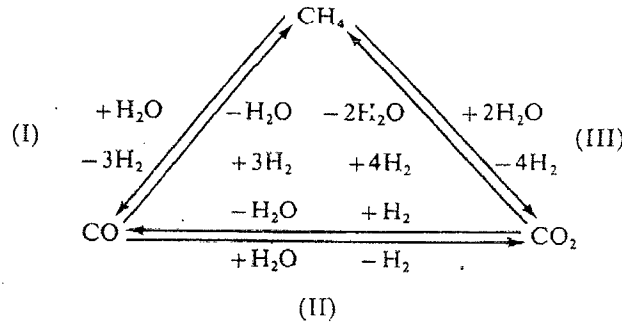


Fig: 4 Mechanism of methane steam reforming reactions (Xu. J, 1989)

$$X_{CH_4} = \frac{C_{CO_2,r} + C_{CO,r}}{C_{CH_4,r} + C_{CO_2,r} + C_{CO,r}} \quad (1)$$

$$R_1 = \frac{\frac{k_1}{P_{H_2}^{2.5}} \left[p_{CH_4} p_{H_2O} - \frac{P_{H_2}^3 P_{CO}}{K_1} \right]}{DEN^2} \quad (2)$$

$$R_2 = \frac{\frac{k_2}{P_{H_2}} \left[p_{CO} p_{H_2O} - \frac{P_{H_2} P_{CO_2}}{K_2} \right]}{DEN^2} \quad (3)$$

$$R_3 = \frac{\frac{k_3}{P_{H_2}^{3.5}} \left[p_{CO} p_{H_2O}^2 - \frac{P_{H_2}^4 P_{CO_2}}{K_3} \right]}{DEN^2} \quad (4)$$

$$p_{CH_4} = (1 - X_{CH_4}) / \sigma \quad (5)$$

$$p_{CO} = (X_{CH_4} - X_{CO_2}) / \sigma \quad (6)$$

$$p_{CO_2} = X_{CO_2} / \sigma \quad (7)$$

$$p_{H_2O} = (m - X_{CH_4} - X_{CO_2}) / \sigma \quad (8)$$

$$p_{H_2} = (p_{H_2}^0 + 3X_{CH_4} + X_{CO_2} - Y_H) / \sigma \quad (9)$$

$$\sigma = (1 + m + p_{H_2O}^0 + 2X_{CH_4} - Y_H) / p_r \quad (10)$$

$$DEN = 1 + K_{CO} p_{CO} + K_{H_2} p_{H_2} + K_{CH_4} p_{CH_4} + K_{H_2O} p_{H_2O} / p_{H_2} \quad (11)$$

Reaction rate terms:

Rate of disappearance of methane (CH₄):

$$R_{CH_4} = (R_1 + R_3) \text{ mol CH}_4 / (\text{kG cat. Sec}) \quad (12)$$

Rate of disappearance of steam (H₂O):

$$R_{H_2O} = (R_1 + R_2 + 2R_3) \text{ mol H}_2\text{O} / (\text{kG cat. Sec}) \quad (13)$$

Rate of formation of Carbon monoxide (CO):

$$R_{CO} = (R_1 - R_2) \text{ mol CO} / (\text{kG cat. Sec}) \quad (14)$$

Rate of formation of Carbon dioxide (CO₂):

$$R_{CO_2} = (R_2 + R_3) \text{ mol CO}_2 / (\text{kG cat. Sec}) \quad (15)$$

Rate of formation of Hydrogen (H₂):

$$R_{H_2} = (3R_1 + R_2 + 4R_3) \pm \frac{\pi D_i L}{Wt} J_{H_2}^{Permeating} \text{ mol H}_2 / (\text{kG cat. Sec}) \quad (16)$$

For co current flow + sign, counter current flow – sign is used.

$$y_H = \frac{F_{H_2}^{P, Out let}}{F_{CH_4}^0} \quad (17)$$

Sievert's law: Permeation flux through the pd-based membrane:

$$J_i^{permeating} = \begin{cases} \frac{Q_0 e^{(-E_p/RT)}}{\delta} \left(\sqrt{P_{H_2}^{Reaction}} - \sqrt{P_{H_2}^{permeation}} \right), & i = H_2 \\ 0 & , i \neq H_2 \end{cases} \quad (18)$$

Ideal Hydrogen recovery yield (y_H) is 4.

2.2 Governing model equations

The isothermal mathematical model is developed to describe the behavior of membrane reactor at steady state based on the following assumptions:

1. Negligible radial temperature/ concentration gradients and isobaric conditions were assumed on the reaction and permeation sides.
2. Permeation flux through the membrane was proportional to the difference of the species partial pressures on the shell and tube sides and the species permeances were assumed independent of temperature in the considered range.
3. Pseudo-homogeneous model was assumed in the catalyst bed.
4. Dispersive flow behavior of reacting components in reaction zone.
5. Plug flow behavior of gas in permeation side.
6. Ideal gas behavior.

With the assumptions specified above, the mass balance equations for components CH_4 , CO_2 , H_2 was written as follows:

MASS BALANCE EQUATIONS:

Reaction side:

Plug flow model:

$$\text{CH}_4 \text{ balance:} \quad \frac{dx_{CH_4}}{dz} = \frac{\rho_c \pi (D_0^2 - D_i^2)}{4F_{CH_4}^0} (R_1 + R_3) \quad (19)$$

Initial condition: At $z = 0$, $x_{CH_4} = 0$;

$$\text{CO}_2 \text{ balance: } \frac{dx_{CO_2}}{dz} = \frac{\rho_C \pi (D_0^2 - D_i^2)}{4F_{CH_4}^0} (R_2 + R_3) \quad (20)$$

$$\text{Initial condition: } \text{At } z = 0, \quad x_{CO_2} = 0;$$

Plug flow reactor model is used to reproduce the proved results and establish new results that are not explained in literature. The same model results are also tested against dispersive flow model. Mass pecllet number which can be expressed as $Pe = uL/D = 0.5$ obtained from literature (Perry's chemical engineering hand book).

Axial Dispersion model:

$$\text{CH}_4 \text{ balance: } \frac{D}{u} \frac{d^2 x_{CH_4}}{dz^2} - \frac{dx_{CH_4}}{dz} + \frac{\rho_C \pi (D_0^2 - D_i^2)}{4F_{CH_4}^0} (R_1 + R_3) = 0 \quad (21)$$

$$\text{Initial condition: } \text{At } z = 0, \quad \frac{D}{u} \frac{dx_{CH_4}}{dz} - x_{CH_4} = 0 \quad (22)$$

$$\text{Boundary condition: } \text{At } z = L, \quad \frac{dx_{CH_4}}{dz} = 0 \quad (23)$$

$$\text{CO}_2 \text{ balance: } \frac{D}{u} \frac{d^2 x_{CO_2}}{dz^2} - \frac{dx_{CO_2}}{dz} + \frac{\rho_C \pi (D_0^2 - D_i^2)}{4F_{CH_4}^0} (R_2 + R_3) = 0 \quad (24)$$

$$\text{Initial condition: } \text{At } z = 0, \quad \frac{D}{u} \frac{dx_{CO_2}}{dz} - x_{CO_2} = 0 \quad (25)$$

$$\text{Boundary condition: } \text{At } z = L, \quad \frac{dx_{CO_2}}{dz} = 0 \quad (26)$$

Above conditions are also known as Danckwerts boundary conditions.

Permeation side:

$$\frac{dy_H}{dz} = \frac{\pi D_i Q_0 e^{(-E_p/RT)} (p_{H_2,r}^{0.5} - p_{H_2,p}^{0.5})}{\delta \cdot F_{CH_4}^0}$$

$$\text{at } z = 0, \quad y_H = 0 \quad (27)$$

For the co current flow simulation, the system of ordinary differential equations is solved using finite difference methods and compared with results obtained by plug flow behavior result

(IVPs) solved through Ruge Kutta 4th order method.

Table 2: Kinetics parameters of methane steam reforming

parameter	Description	Units	Pre exponential factor	Activation energy (kJ/mol)
k ₁	Reaction 1	(mol.pa ^{0.5} /(kg cat.S))	3.7113*10 ¹⁷	240.1
k ₂	Reaction 2	(mol/(kg cat. Pa. S))	5.4306	67.13
k ₃	Reaction 3	(mol.Pa ^{0.5} /(kg cat.S))	8.9598*10 ¹⁶	243.9
K ₁	Equilibrium1	(Pa ²)	5.75*10 ²²	95.411464
K ₂	Equilibrium2	-	0.0126	-38.568646
K ₃	Equilibrium3	(Pa ²)	7.24*10 ²⁰	179.964844
K ₄	CH ₄ Adsorption	(Pa ⁻¹)	6.65*10 ⁻⁹	-38.28
K ₅	H ₂ O Adsorption	-	177000	88.68
K ₆	H ₂ Adsorption	(Pa ⁻¹)	6.12*10 ⁻¹⁴	-82.9
K ₇	CO Adsorption	(Pa ⁻¹)	8.23*10 ⁻¹⁰	-70.65
Q	H ₂ Permeation	(mol/(M.S.Pa ^{0.5}))	6.9643*10 ⁻⁷	15.7

Table 3: Reactor specifications (Shu et al, 1994)

Reactor Specification	Value
Inner diameter (D _i)	0.0095 M
Outer diameter (D _o)	0.017 M
Length (L)	0.036 M
Reaction zone pressure (P _r)	136000 Pa
Permeation zone pressure (P _p)	101325 Pa
Operating temperature (T _r)	773K
Steam to methane ratio (m)	3
Methane flow rate (F _{A0})	42 ml/min (SCCM)
Sweep factor (I)	1
Membrane thickness	20 μM

The advantage of using a membrane reactor is demonstrated by the following facts. The removal of hydrogen from the reaction zone increases the methane conversion. The reaction may consequently be carried out at a lower temperature. Besides an increased conversion of methane at lower temperatures, the removal of hydrogen from the reaction gas influences the potential for carbon formation.

The only way to drastically increase the permeation rate is to decrease the membrane thickness. In a catalytic system the risk of carbon formation is normally evaluated by means of the 'principle of equilibrated gas' which state that carbon formation can be expected if the gas shows affinity for carbon formation after the establishment of the reforming (i) and shift equilibrium (ii)

Results And Discussion

Results and discussion:

The validation of the model was made by means of numerical results with experimental data available in literature namely those by Shu et al 1994, and Giuseppe 1997. They studied the methane steam reforming process in a catalytic membrane reactor using a Stainless Steel supported Pd membrane. It is possible to observe a good agreement between experimental and simulation results.

Effect of various parameters:

Here in this work, the independent parameters on which the conversion of Methane, carbon dioxide and permeation of hydrogen are depending identified initially, and the effects of those parameters on these parameters are calculated numerically through appropriate numerical technique. (Implicit Finite difference methods, Runge kutta 4th order method).

Only Conversions of CH₄, CO₂ and permeation of H₂ are taken into account because all other parameters can be expressed as constitutive relationships of these parameters.

Main independent parameters on which the above stated terms are depending covered in this work are,

1. Temperature
2. Reaction zone pressure
3. Flow rate of reactant species
4. Steam to methane ratio
5. Sweep factor
6. Catalyst weight
7. Membrane thickness
8. Reactor length

3.1 Effect of Temperature:

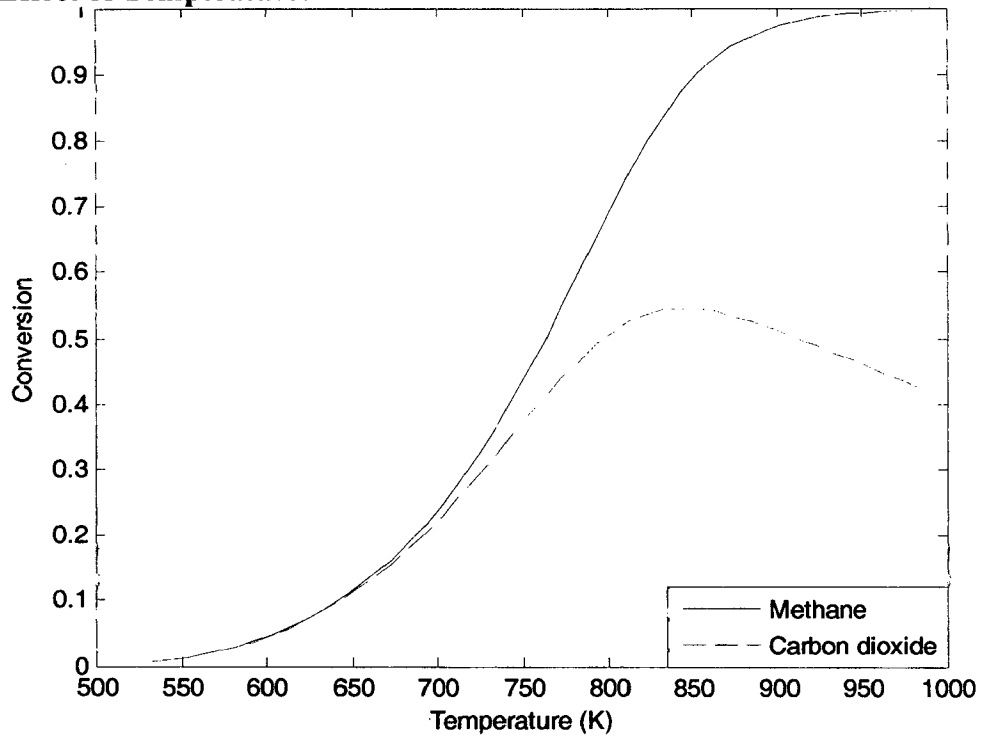


Fig: 5 Temperature effect on conversions of CH₄, CO₂ in PFR model

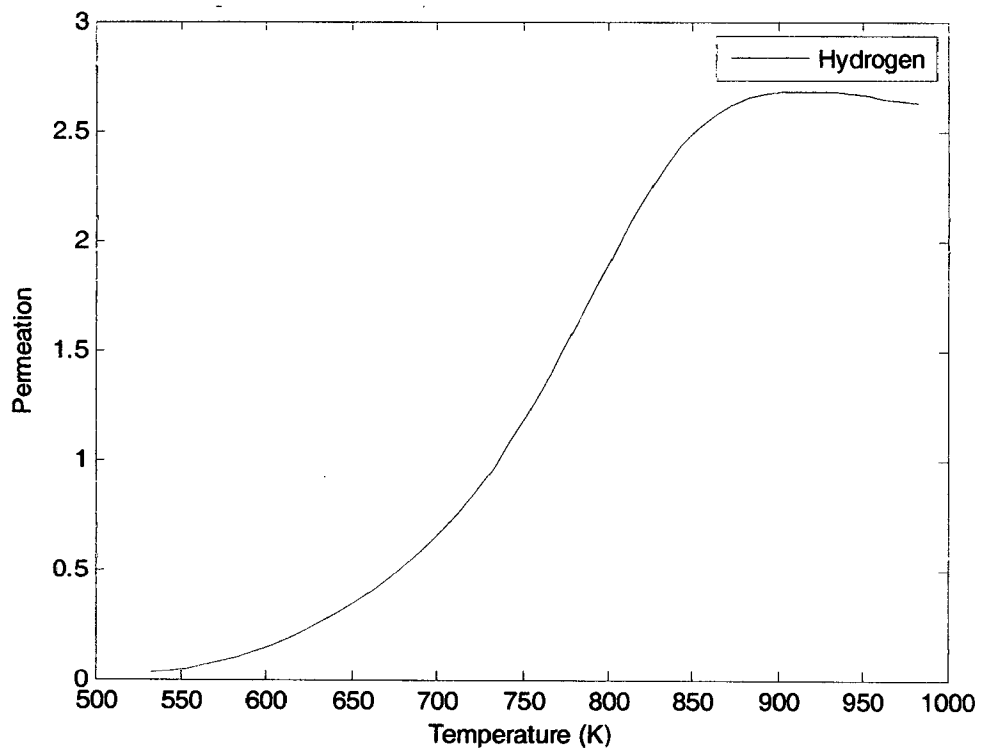


Fig: 6 Effect of Temperature on H₂ recovery yield in PFR model

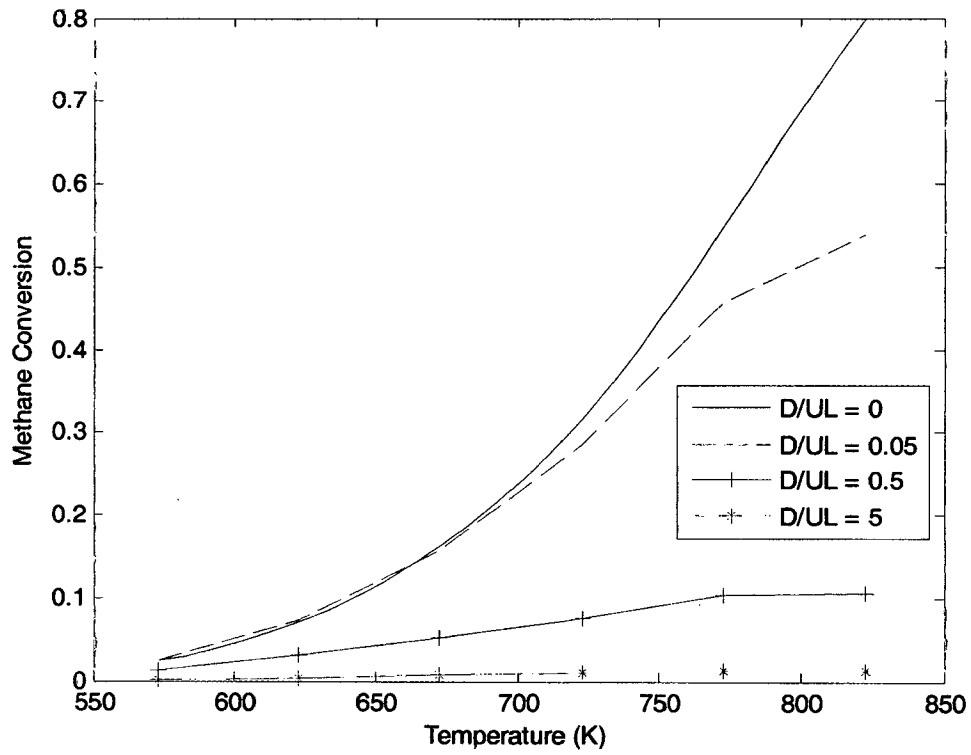


Fig: 7 Effect of Temperature on CH₄ conversion in axial dispersion model

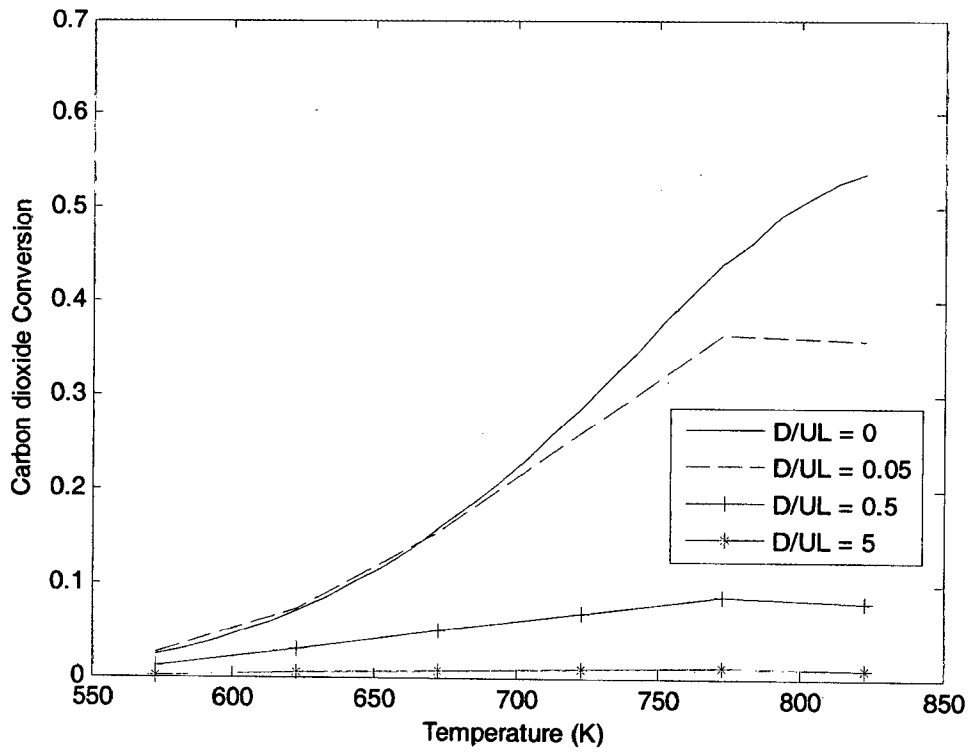


Fig: 8 Effect of temperature on CO₂ conversion in axial dispersion model

Reaction temperature plays an important role in the reactor performance through

thermodynamics and kinetics. In the case of methane steam reforming, the use of a membrane reactor can lead to a significantly enhanced methane conversion at a moderate temperature. In our study, the temperature effect was calculated using the kinetic permeation model for the Pd/SS membrane. Under the above mentioned reaction conditions, methane conversions in membrane reactor at various temperatures were predicted, as shown in Fig 5. When methane steam reforming was performed in the palladium membrane reactor without a catalyst, no detectable conversion occurred at 777 K, which might be due to the low specific surface area of the membrane as well as its limited intrinsic catalytic activity. Thus a catalyst was necessary to perform effectively the reforming reaction. High temperature and low pressure thermodynamically favor the process because of the endothermic nature of the reaction and the fact that it is also characterized by an increase in the number of moles.

It can be seen that the methane conversion and the hydrogen recovery yield increase with the reaction temperature due to the endothermic nature of reaction system, and their values in the membrane reactor (0.5483 at 773K) are much larger than the equilibrium values (0.39 at 773K) (Shu et al 1994). The same trend is also observed in axial dispersion model for different dispersive coefficient values. The results also show that the influence of reaction temperature on the membrane reactor performance becomes less with the increase in temperature. At 850 K, the conversion of methane almost reaches 1.0. The reactor performance could not be further improved by increasing the reaction temperature. However, the reaction temperature still influences the equilibrium values significantly at higher temperature. Therefore, the improvement in conversion for the membrane reactor over the corresponding equilibrium value becomes slighter at higher temperature.

3.2 Effect of Reaction zone pressure:

Fig. 9 shows the effect of the reaction pressure on the level of methane conversion, with the permeation side at atmospheric pressure. Since the steam reforming of methane is accompanied by a volume expansion (net increase of moles on the product side), lower reaction pressures are thermodynamically favored. The equilibrium conversion decreases with increasing reaction pressure. In the palladium membrane reactor, the level of methane conversion increased with increasing reaction pressure. Although a high reaction pressure depletes the steam reforming conversion equilibrium, the increase of hydrogen partial pressure on the reaction side would increase the driving force for hydrogen permeation, resulting in an enhancement of the methane conversion under certain conditions. Reaction pressure can influence either the rate of hydrogen

production or that of hydrogen permeation. Pressure had a positive effect on the hydrogen yield because of the increase in driving force for the permeance of hydrogen. The yield of hydrogen increased with pressure and reached a value which is 108% than the value obtained for the equilibrium yield (equilibrium in Shu et al 1994). The membrane reactor with dispersive flow has a similar increasing trend with increasing pressure are shown in figure 11, 12.

An increase of the total pressure results in an increase of the partial pressure of hydrogen, thereby helping the membrane to remove hydrogen down to a lower H/C ratio of the process gas, which results in a higher methane conversion.

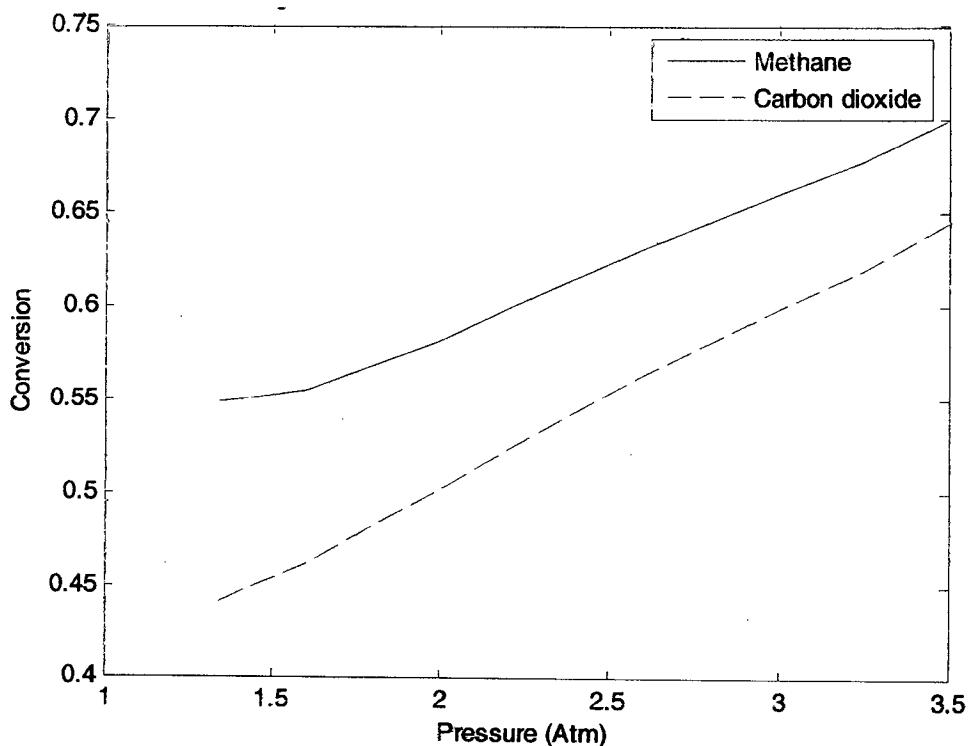


Fig: 9 Effect of pressure on CH₄, CO₂ conversions in PFR model at 773 K

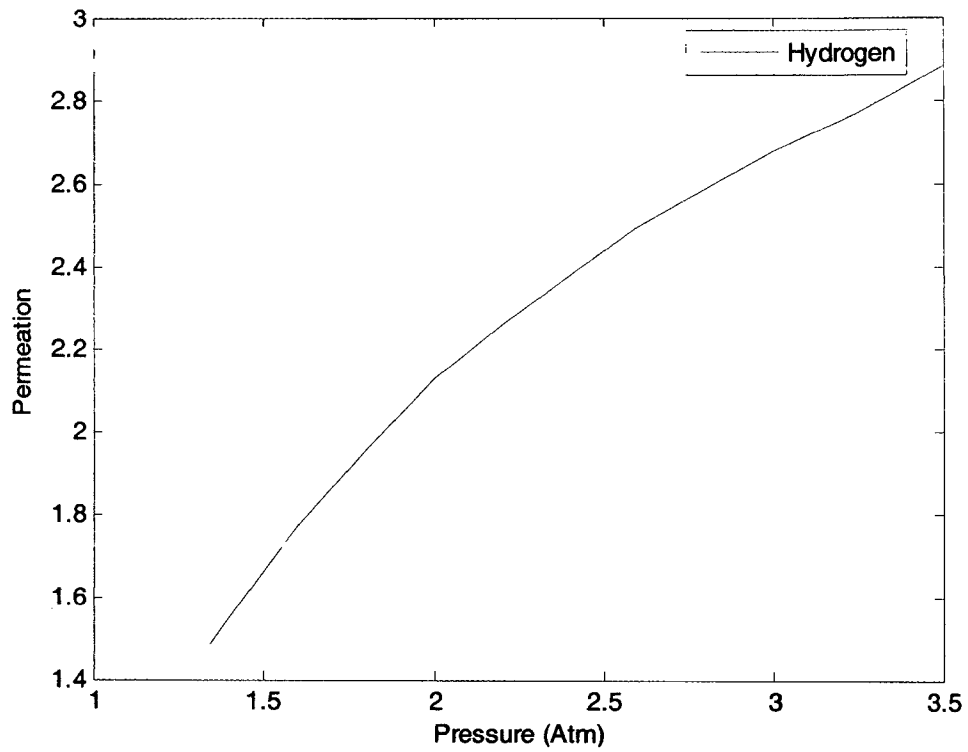


Fig: 10 Effect of pressure on H₂ recovery yield in PFR model at 773 K

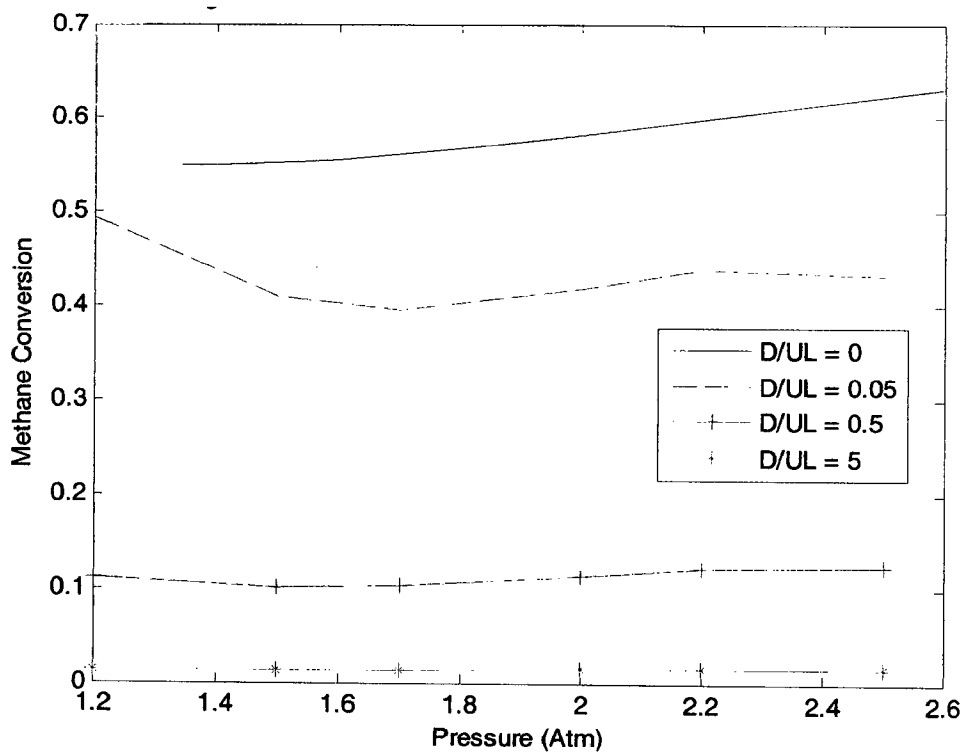


Fig: 11 Effect of pressure on CH₄ conversion in axial dispersion model at 773 K

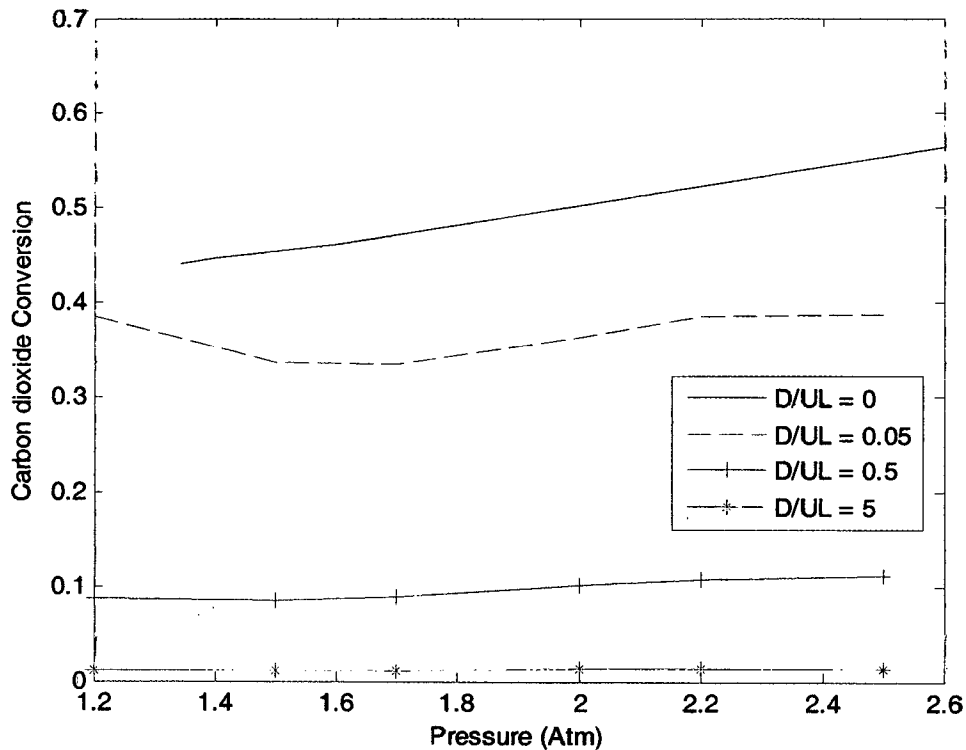


Fig: 12 Effect of pressure on CO₂ conversion in axial dispersion model at 773 K

Uemiya et al. noticed a conversion increase with increasing reaction pressure. We also calculated the dependence of methane conversion on the total pressure under various purging conditions for a palladium membrane of 20 μM thick. It was found that the increasing tendency exists in the case where hydrogen separation is efficient. The permeance of hydrogen is not high enough to overcome the effect of thermodynamics due to the increase in moles in the reaction. However, permeance increases at higher pressures because of the increase in driving force.

3.3 Effect of Reactants flow rate:

The effect of reactants flow rate on methane conversion was examined by varying this ratio from 42 to 200 SCCM, keeping the steam to methane ratio and sweep factor constant. So increasing the feed flow rate means increment in reactant initial concentration. The results obtained at 773 K are drawn in Fig. 13 and 14. CH₄ and CO₂ conversions are exhibiting monotonic decrease with the flow rate. The hydrogen recovery yield is also showing the same trend. As the residence time for the reaction is reduced when the total feed flow rate increases, this kind of plots are obtained. But a different kind of profile was observed in dispersion model. It could be mainly due to the non ideal behavior of the reactants stream.

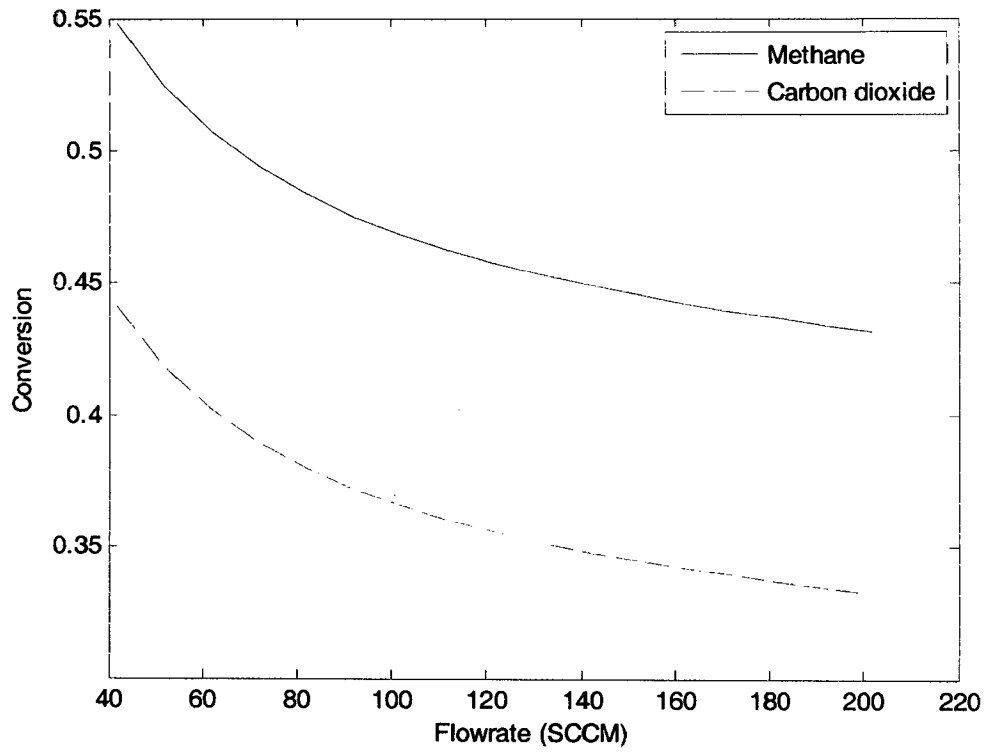


Fig: 13 Effect of reactants flow rate on CH₄, CO₂ conversions in PFR model at 773 K

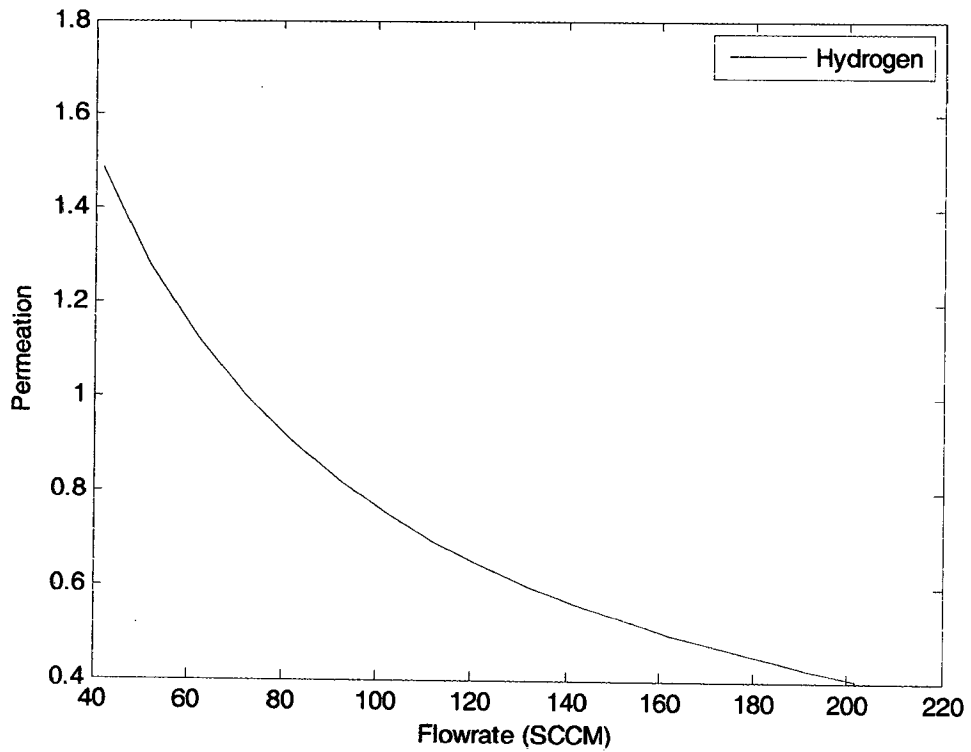


Fig: 14 Effect of reactants flow rate on H₂ recovery yield in PFR model at 773 K

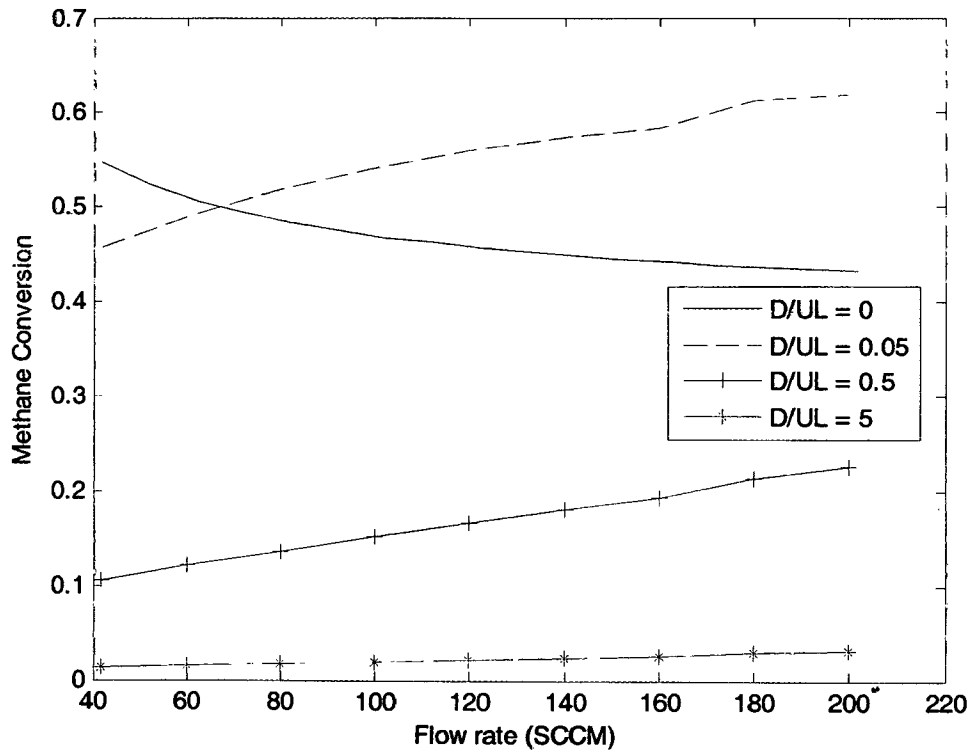


Fig: 15 Effect of reactants flow rate on CH₄ conversion in axial dispersion model at 773 K

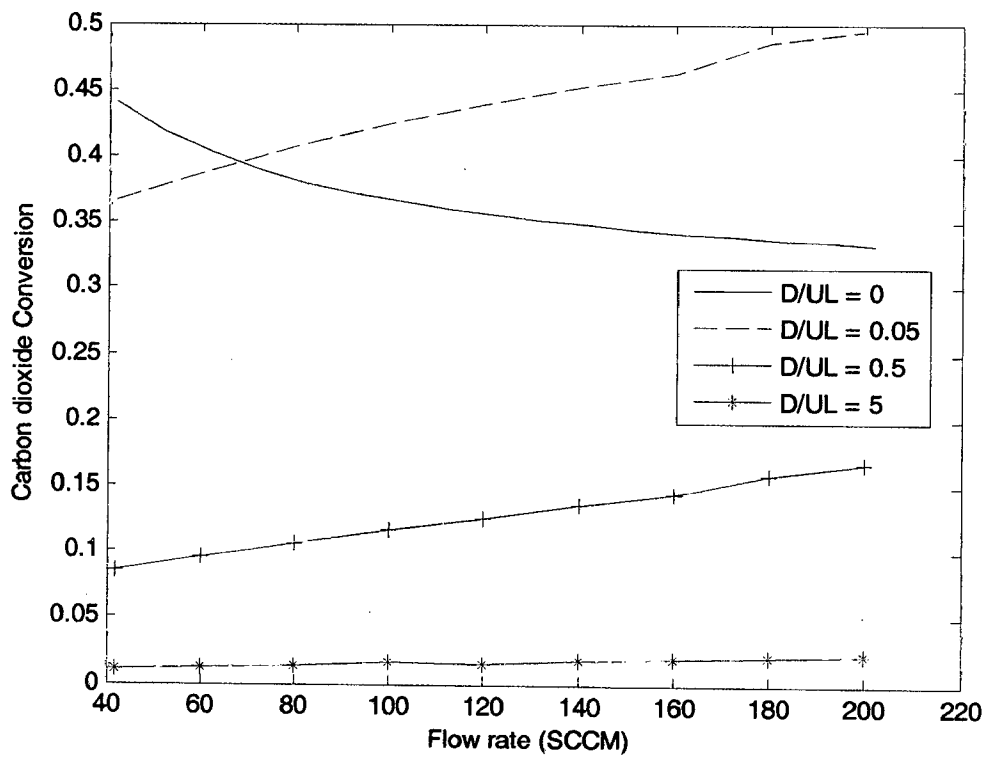


Fig: 16 Effect of reactants flow rate on CO₂ conversion in axial dispersion model at 773 K

3.4 Effect of Steam to Methane ratio (m):

Methane steam reforming usually proceeds in the presence of an excess of steam to prevent the carbon deposition over the catalyst surface and to enhance the steam reforming. The effect of molar steam to methane ($\text{H}_2\text{O}/\text{CH}_4$) ratio on methane conversion was examined by varying this ratio from 1 to 12 and keeping the methane feed flow rate constant. So increasing the feed ratio means increment in total feed flow rate. The results obtained at 773 K are drawn in Fig. 17. CH_4 , CO_2 conversions are exhibiting monotonic increase with the steam-to-methane ratio. But the hydrogen recovery yield first increases to a maximum value, but then decreases (Fig 18). In general, increasing the feed ratio gives rise to an enhancement in methane conversion and therefore should improve the hydrogen recovery yield by reducing the unconverted methane. On the other hand, the increase in feed ratio causes a decrease in the driving force for the hydrogen permeation. The amount of hydrogen permeated is reduced at higher feed ratio due to the decrease in hydrogen mole fraction and therefore the partial pressure on the reaction side because of the reduced hydrogen partial pressure on the reaction side, the recovery yield will be reduced.

In the case of the Pd/SS membrane, an enhancement of the membrane separation efficiency was realized by continually pumping the permeation side (tube side) with a rotary vacuum pump. The pumping eliminated the radial distribution of the hydrogen concentration inside the support pores and kept the permeation side under a low pressure, resulting in a relatively high driving force of hydrogen permeation through the palladium membrane. It is clear that the methane conversion was greatly enhanced in this manner. In this case, helium passed through the permeation side at a flow-rate of 42 SCCM. The promotion of the reforming conversion is clearly exhibited.

It has earlier been reported (Laegsgaard 1995) that a steam to carbon ratio of 2.5 is sufficient to avoid the formation of carbon. Increasing the steam/carbon ratio beyond 2.5 increases the rate of hydrogen production but also dilutes the hydrogen in the retentate stream due to the higher steam content. The latter effect is dominant and the driving force for hydrogen permeation through the membrane is lower in the complete length of the reactor. Hence, a larger membrane area is needed if the S/C ratio is increased.

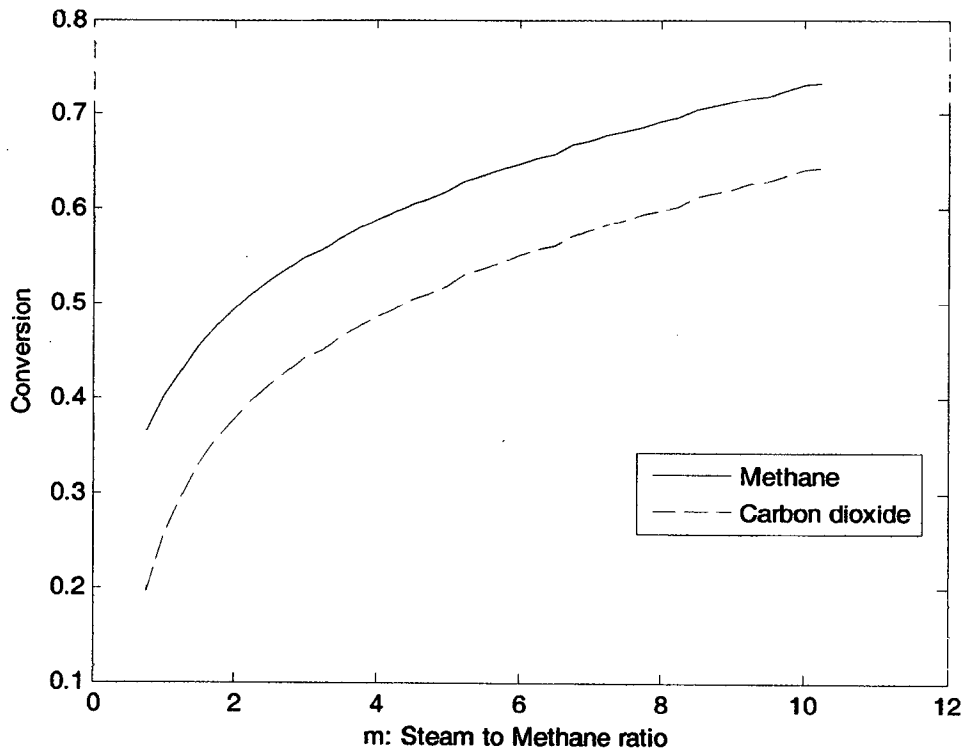


Fig: 17 Effect of Steam to methane ratio on CH_4 , CO_2 conversions in PFR model at 773 K

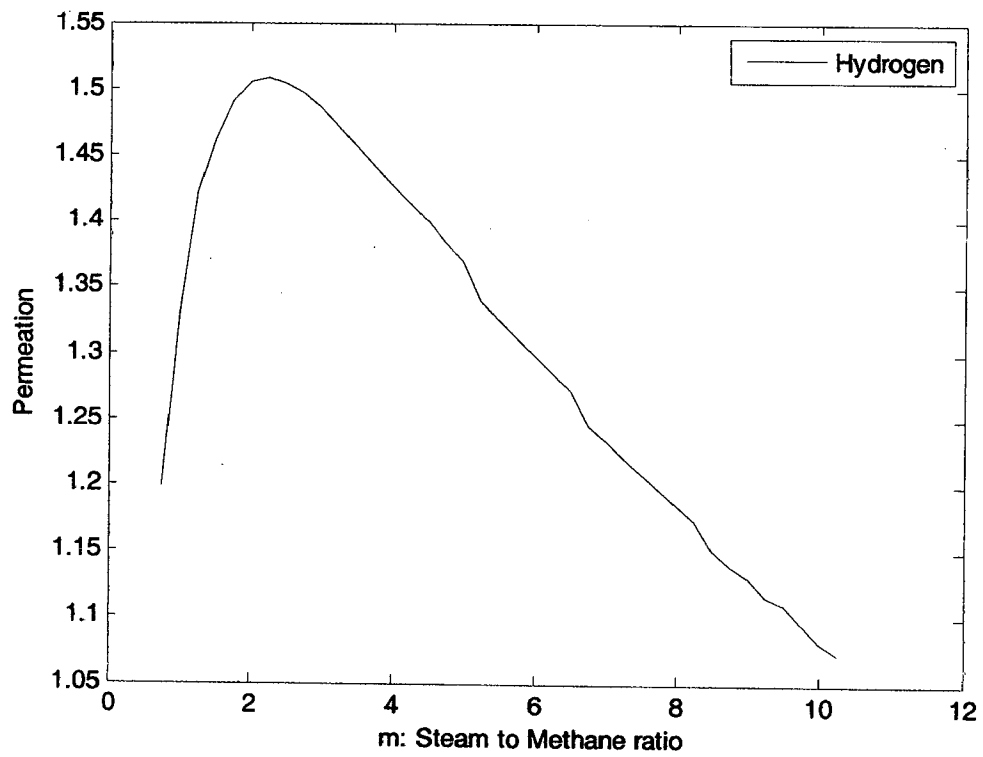


Fig: 18 Effect of Steam to methane ratio on H_2 recovery yield in PFR model at 773 K

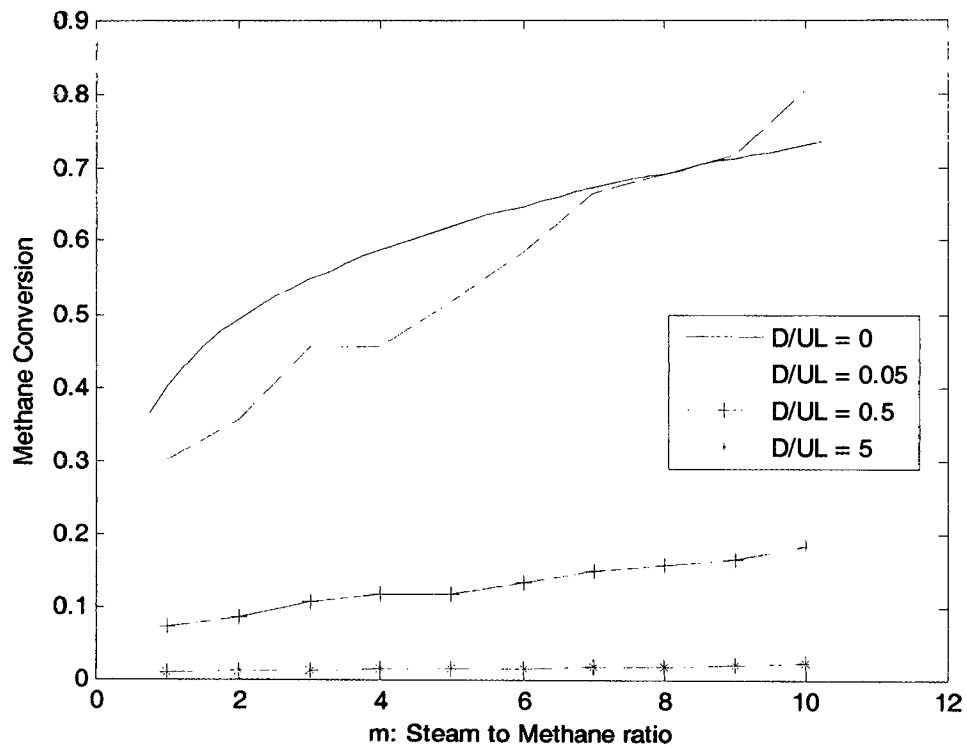


Fig: 19 Effect of Steam to methane ratio on CH₄ conversion in axial dispersion model at 773 K

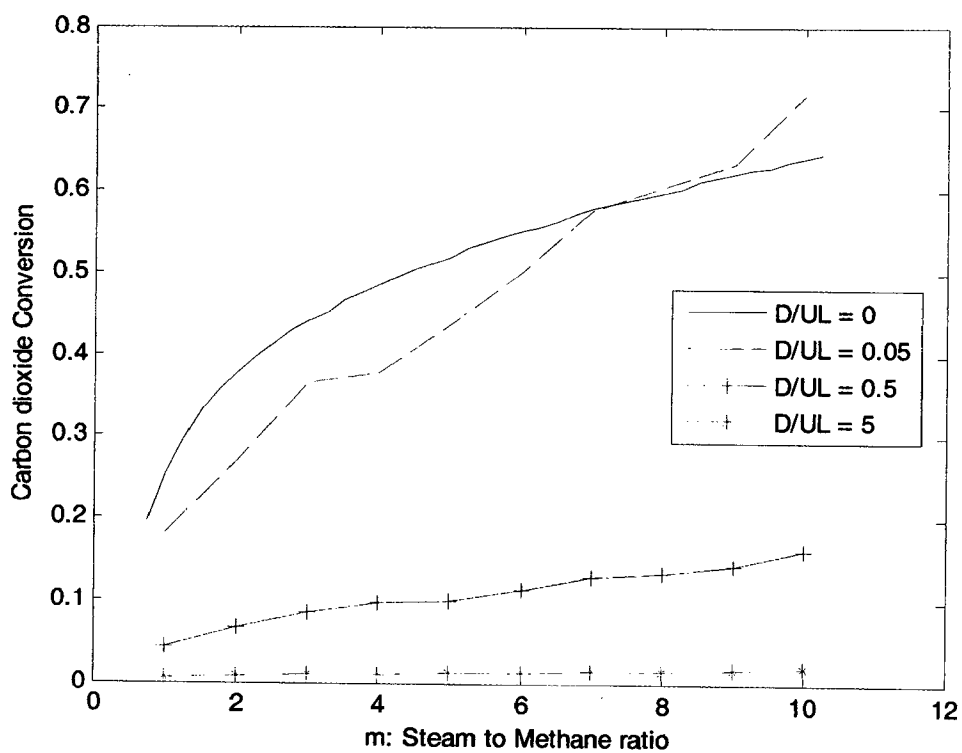


Fig: 20 Effect of steam to methane ratio on CO₂ conversion in axial dispersion model at 773 K

By forcing hydrogen extraction from the catalytic bed, carbon deposition is favored. Although

these conditions lead to a fast growth of carbon filaments in conventional reforming catalysts such as $\text{Ni}/\text{Al}_2\text{O}_3$, in catalysts such as $\text{Ni}/\text{Ce}_{0.5}\text{Zr}_{0.5}\text{O}_2$, no carbon deposition is observed (Shu et al 1994). The use of high oxygen mobility supports, such as Ce-Zr mixed oxides, to disperse the nickel phase results in highly efficient catalysts capable of keeping their surface free from inactive carbon deposits.

3.5 Effect of sweep factor:

At constant pressure, the final equilibrium state of a reacting system depends only on initial conditions (e.g., reactant molar ratio) and the final temperature. For a membrane reactor, the initial conditions also include the sweep factor (I). Chemical potential gradient of permeation component depends on the sweep factor, I.

Sweep factor (I) = the ratio between sweep gas and reference reactant flow rates

The effect of Sweep factor (I) on methane conversion was examined by varying this ratio from 1 to 7 and keeping the methane feed flow rate constant. So increasing the sweep factor means increment in sweep gas (He) flow rate. The results obtained at 773 K are drawn in Fig. 21. CH_4 , CO_2 conversions in membrane reactor are increasing functions of the sweep factor. Purging the permeation side is important in maintaining a high hydrogen partial pressure difference between the two sides of the membrane and moving out hydrogen product from the reaction system. As discussed above, the increase of the purge gas flow rate is expected to enhance the methane conversion owing to the decrease of the hydrogen partial pressure on the permeation side. This effect was examined in the Pd/SS membrane system, as shown in Fig. 21 (Curve 1). The methane conversion was found slightly increased with raising the purge gas flow-rate. The effect reported by Uemiya et al. 1991 is also lower than the calculated purge effect for the same reaction under similar conditions. This may imply that there is a great potential to improve the membrane separation efficiency. In our model, the higher the flow-rate of the purge gas, the more the measured methane conversion. This was quite possibly caused by the cooling effect of the purge gas stream as well as the oversimplified boundary layer condition. In general, increasing the purge gas flow-rate enhances the hydrogen separation efficiency. However, the economy in a large scale industrial application may not permit the use of large amounts of inert gas. Instead, in the case of methane steam reforming, steam may be used as the purge gas. This would also make the subsequent separation of hydrogen from the purge stream much easier since steam can be easily condensed from the mixture. The behaviors of different reactors were compared at the same feed conditions and at different sweep gas flow rates.

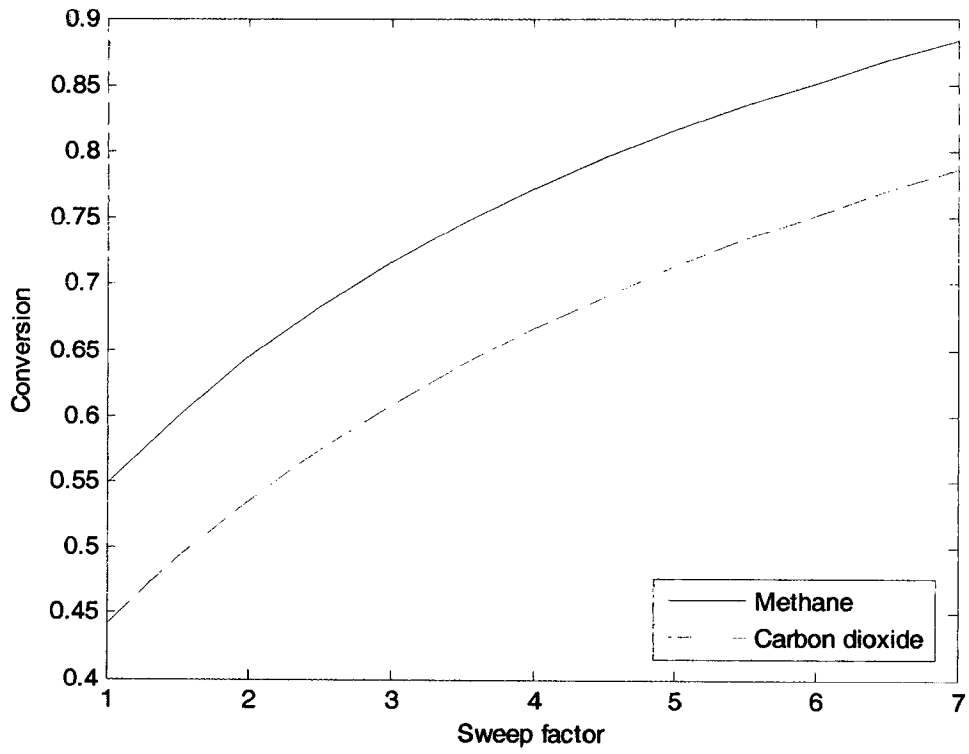


Fig: 21 Effect of sweep factor on CH₄, CO₂ conversions in PFR model at 773 K

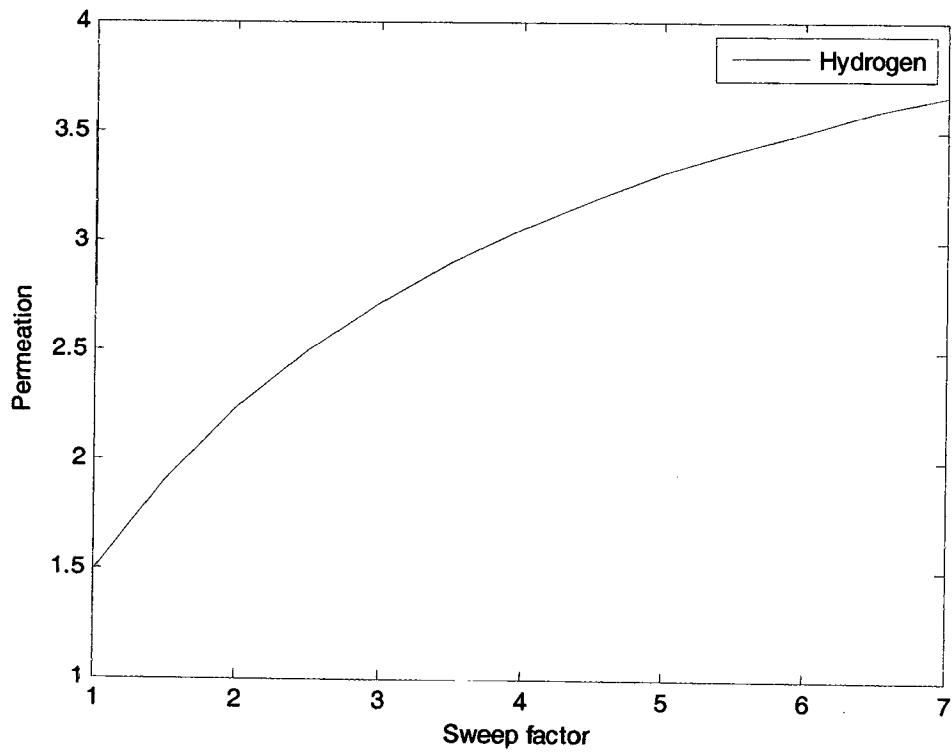


Fig: 22 Effect of sweep factor on H₂ recovery yield in PFR model at 773 K

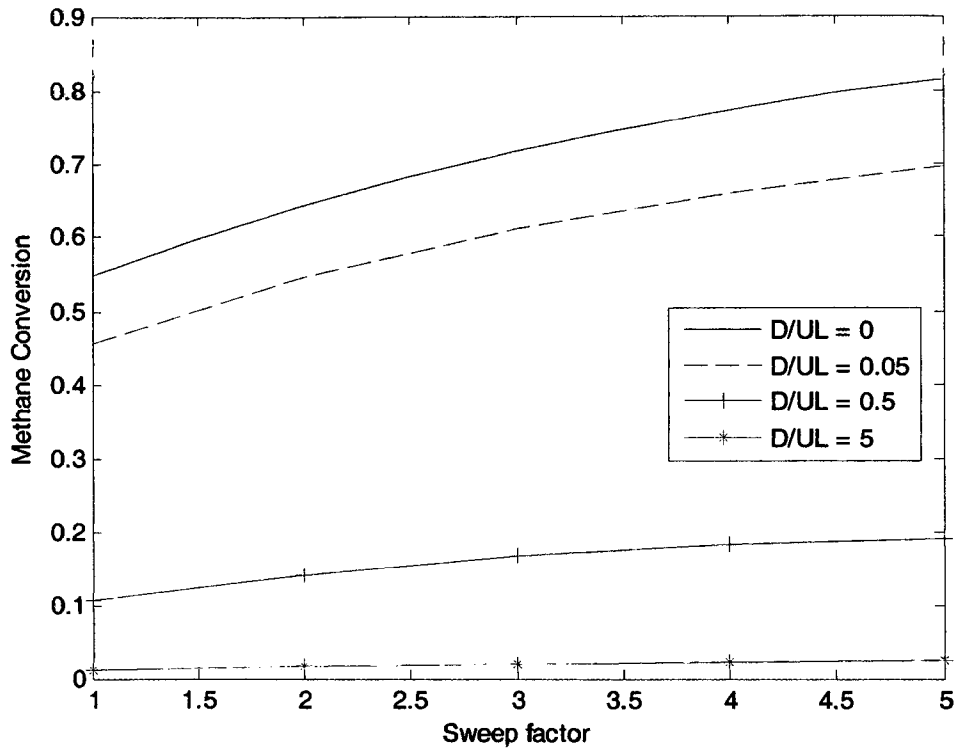


Fig: 23 Effect of sweep factor on CH₄ conversion in axial dispersion model at 773 K

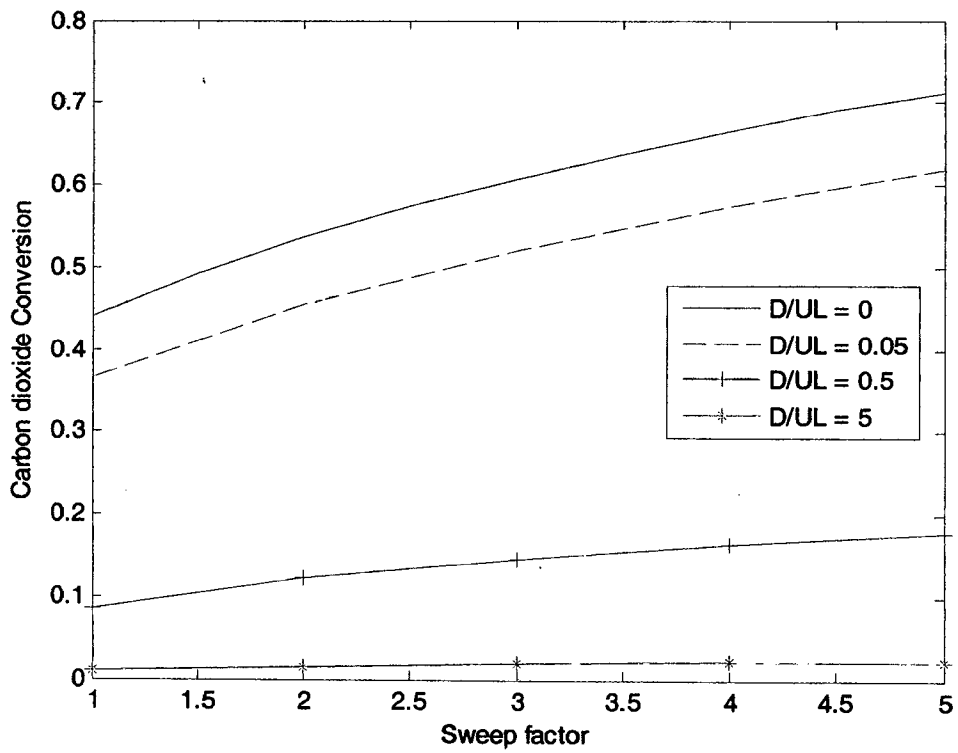


Fig: 24 Effect of sweep factor on CO₂ conversion in axial dispersion model at 773 K

The effect of dispersion coefficient on conversion vs sweep factor is also shown above for CH₄

and CO₂. The expected conversion decreases with increase in dispersion coefficient value due to the non ideal nature of the reaction zone.

3.6 Effect of catalyst weight:

The effect of catalyst weight on methane conversion was examined by varying this value from 1 to 20 gm and keeping the volume of reaction constant. So increasing the catalyst weight means increment in catalyst density. The results obtained at 773 K are drawn in Fig. 25. The equilibrium conversions (CH₄, CO₂) of a membrane reactor are increasing functions of the catalyst weight. For a fixed temperature the conversion of components achieves a final value after which it is not possible to increase. This is because of the endothermic nature of the reaction. One can increase this extent of conversion to more value by increasing temperature.

In the same manner, permeation of H₂ can also be explained. The H₂ recovery yield increases with increase in catalyst weight and approaches a final steady value at that temperature, beyond which it can be improved only by increment in its temperature.

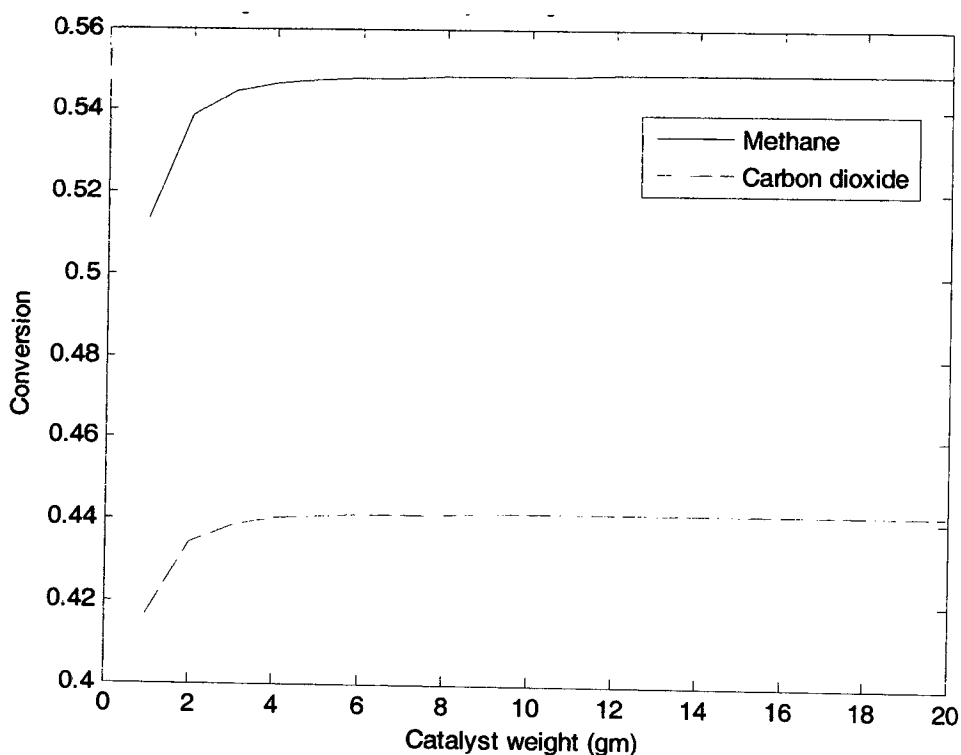


Fig: 25 Effect of catalyst weight on CH₄, CO₂ conversion in PFR model at 773 K

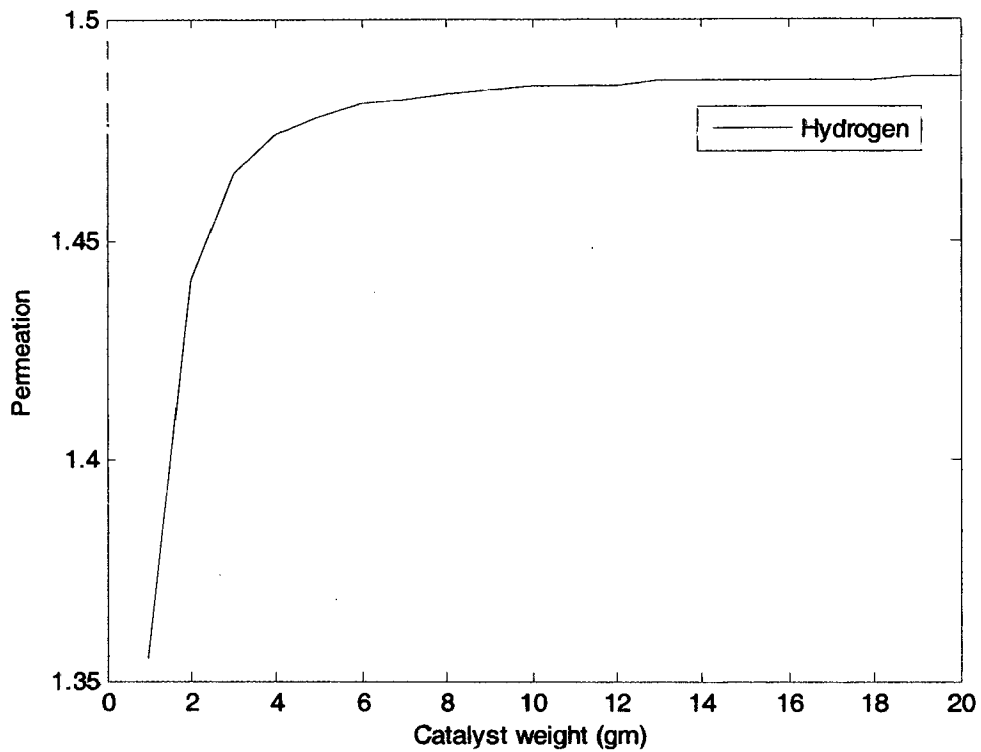


Fig: 26 Effect of catalyst weight on H₂ recovery yield in PFR model at 773 K

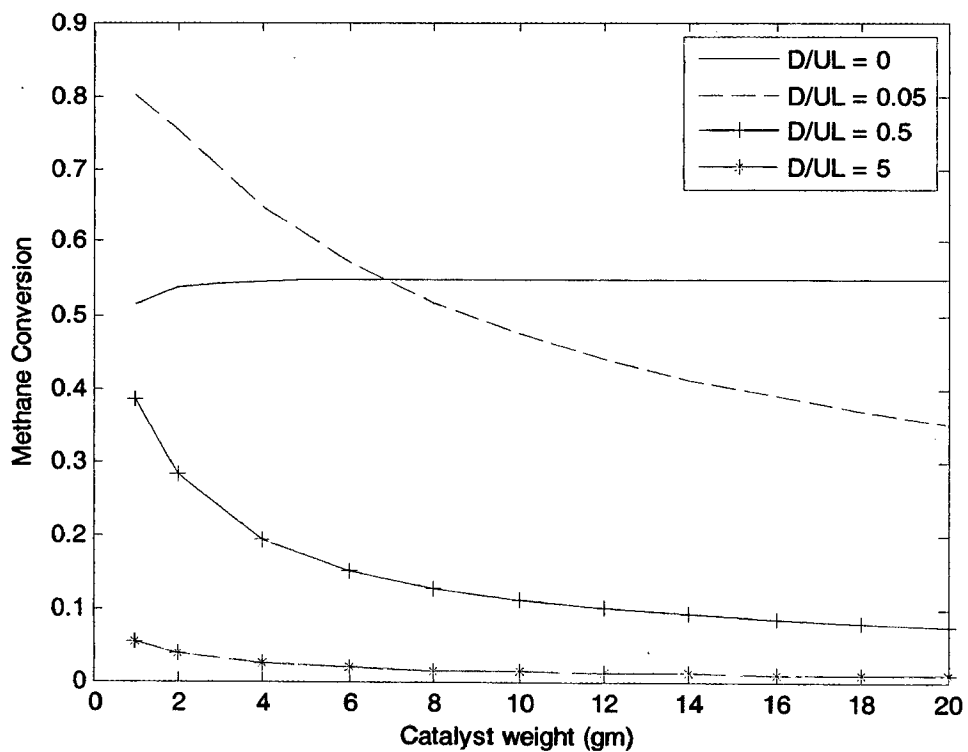


Fig: 27 Effect of catalyst weight on CH₄ conversion in axial dispersion model at 773 K

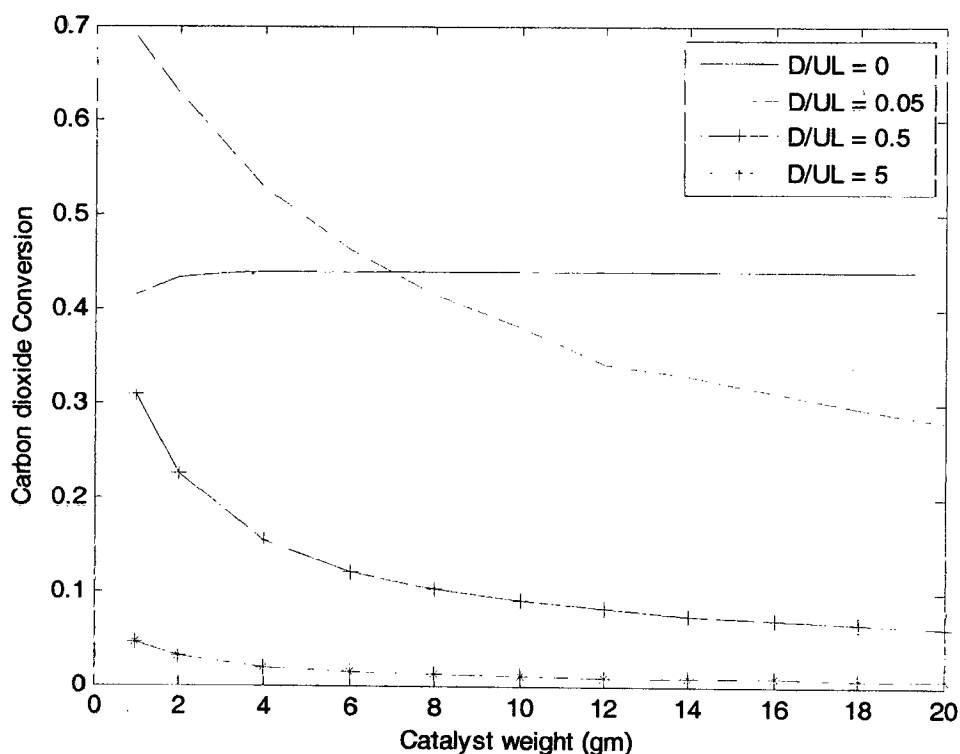


Fig: 28 Effect of on CO₂ conversion in axial dispersion model at 773 K

But due to the non ideal nature of the reaction zone which is considered in this work the dispersive model has produced different kind of results. Though the final achievable conversion value would be lesser compared to that one of PFR model, the initial result obtained is more. It is because the hydrogen separation ratio decreases with an increase in the catalyst weight.

3.7 Effect of Membrane thickness increment:

When the film thickness is increased, selectivity for hydrogen separation improves and the appearance of pinholes during heat treatment is avoided, but apart from its higher cost, the hydrogen permeability and the module capacity decrease and reduce the reactor performance.

The methane conversion was higher in the membrane reactor than in the traditional one. An indirect consequence should be that the membrane reactor could give the same methane conversion as the traditional reactor but operating at a lower temperature. Although dense palladium membrane reactors give, the highest methane conversions compared to composite membrane reactors, dense membranes are characterized by hydrogen permeabilities that are lower than those in composite micro porous membranes are. In this context, the thickness of palladium layer deposited inside a ceramic support is an important calibrating parameter to

optimize the reaction system. As increasing the thickness of palladium layer could shift the behavior of the membrane from the higher to the lower hydrogen permeability zone, the methane conversion varies from higher to lower values.

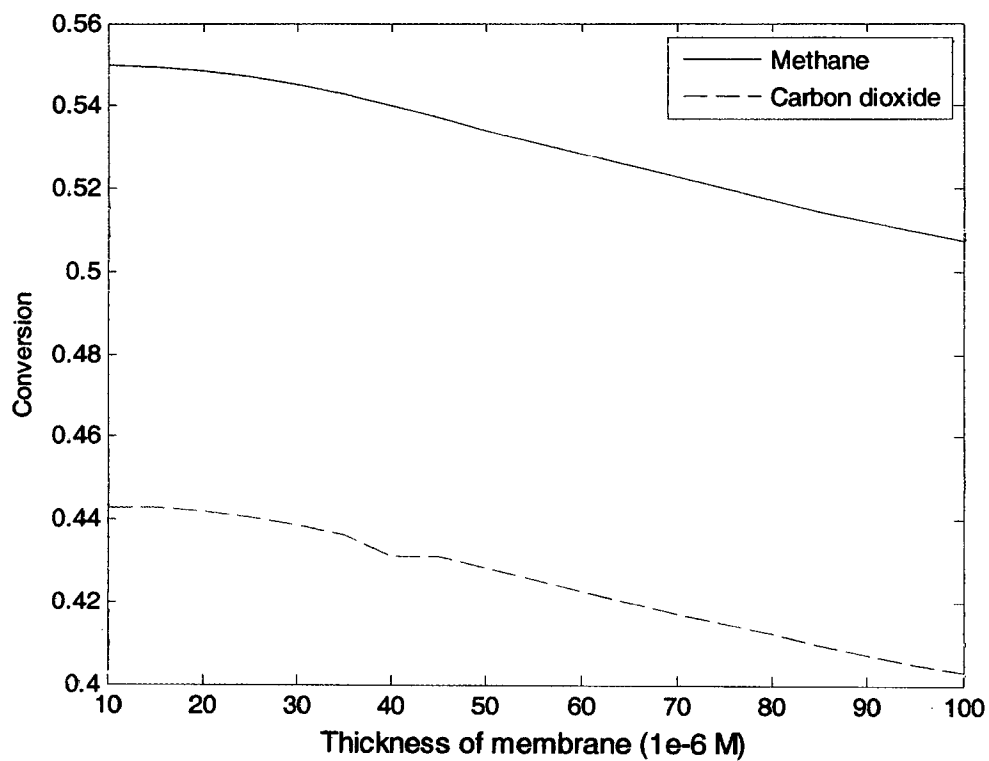


Fig: 29 Effect of membrane thickness on CH₄, CO₂ conversions in PFR model at 773 K

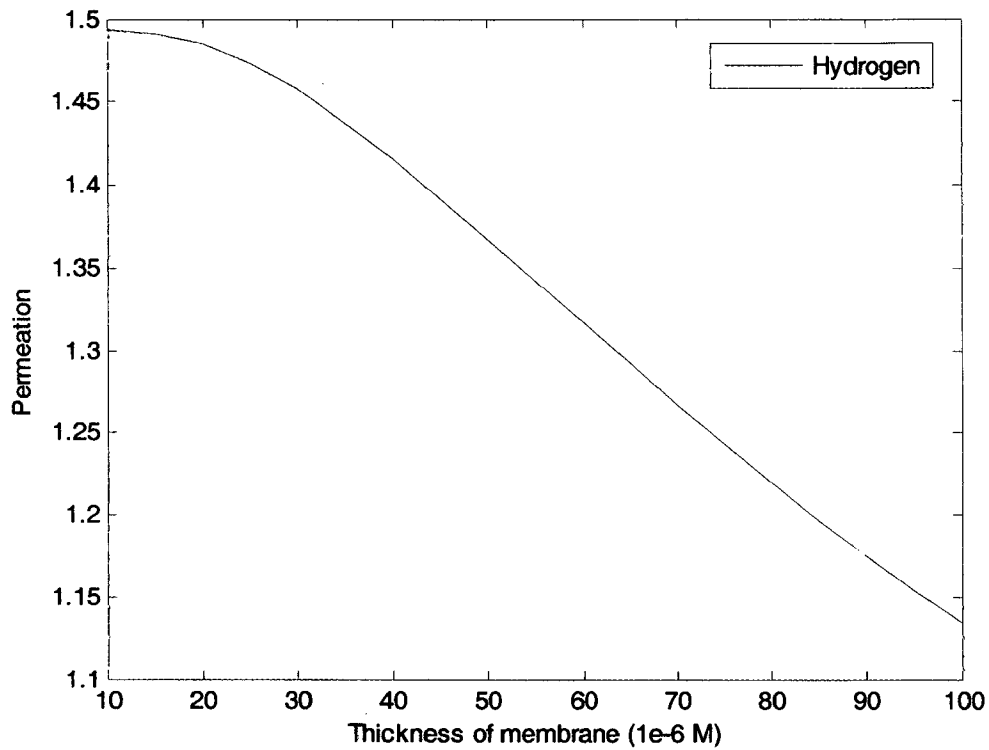


Fig: 30 Effect of Membrane thickness on H_2 recovery yield in PFR model at 773 K

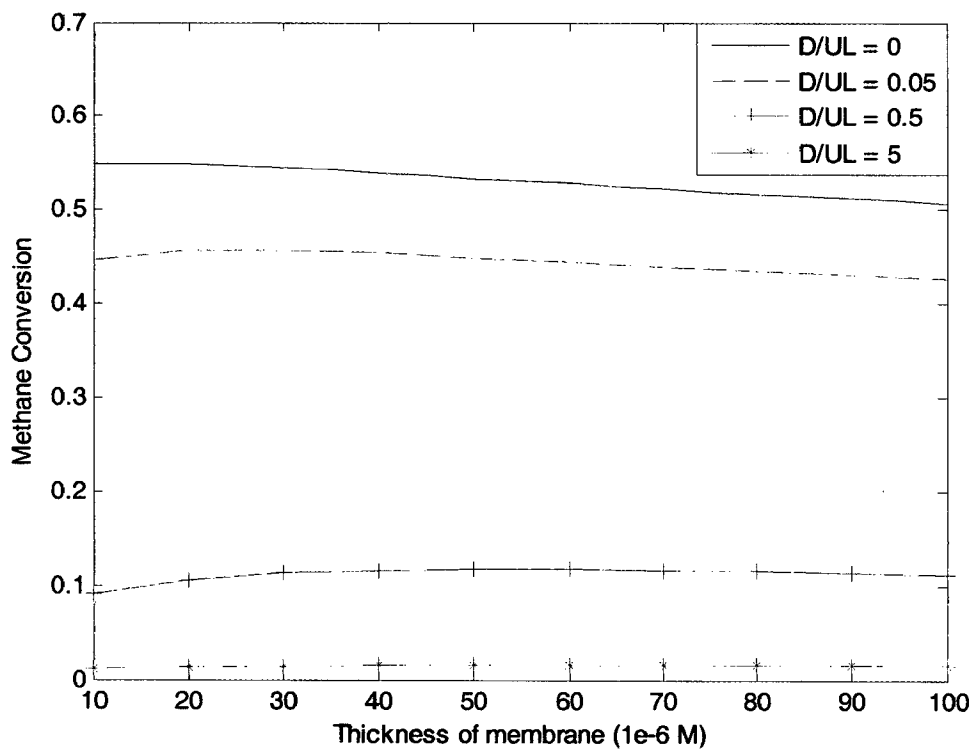


Fig: 31 Effect of membrane thickness on CH_4 conversion in axial dispersion model at 773 K

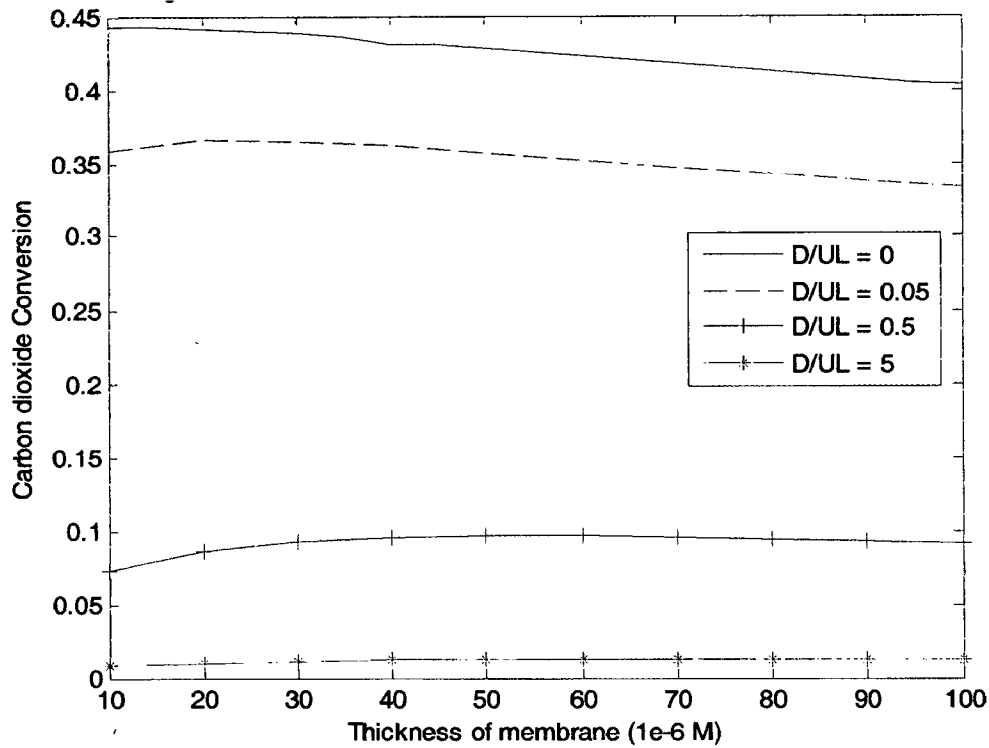


Fig: 32 Effect of Membrane thickness on CO₂ conversion in axial dispersion model at 773 K

Similar types of profiles are observed in dispersive flow model results. As the dispersion coefficient increases the non ideal nature increases and the achievable conversions decrease.

3.8 Effect of reactor length:

The effect of reactor length on methane conversion was examined by varying this value from 0 to 0.036 M and keeping the other parameters constant. So increasing the reactor length means increment in total volume of reaction. The results obtained at 773 K are drawn in Fig: 33, 34, 35 and 36. All parameters (conversions and permeation) are exhibiting monotonic increase with the reactor length.

Results obtained from both models are presented in the following figures. The predicted conversions from the model are comparably low in axial dispersion model. This is due to the non ideal nature of the reaction mixture. So it is suggested always that operational strategy should be such that the reactor would achieve ideal model.

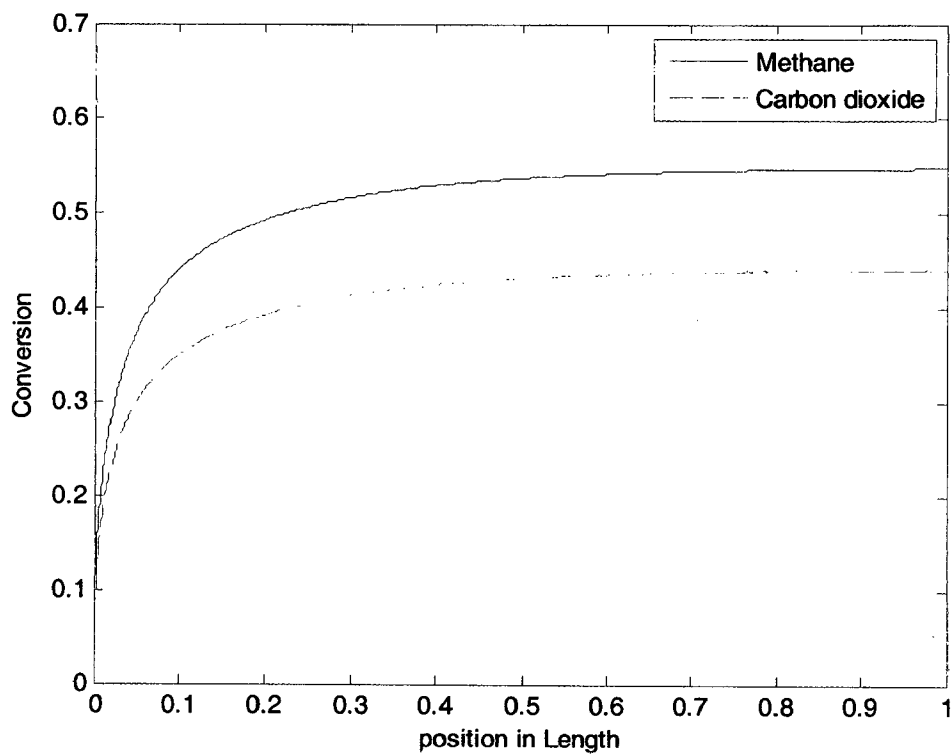


Fig: 33 Effect of reactor length on conversions of CH₄, CO₂ in PFR model at 773 K

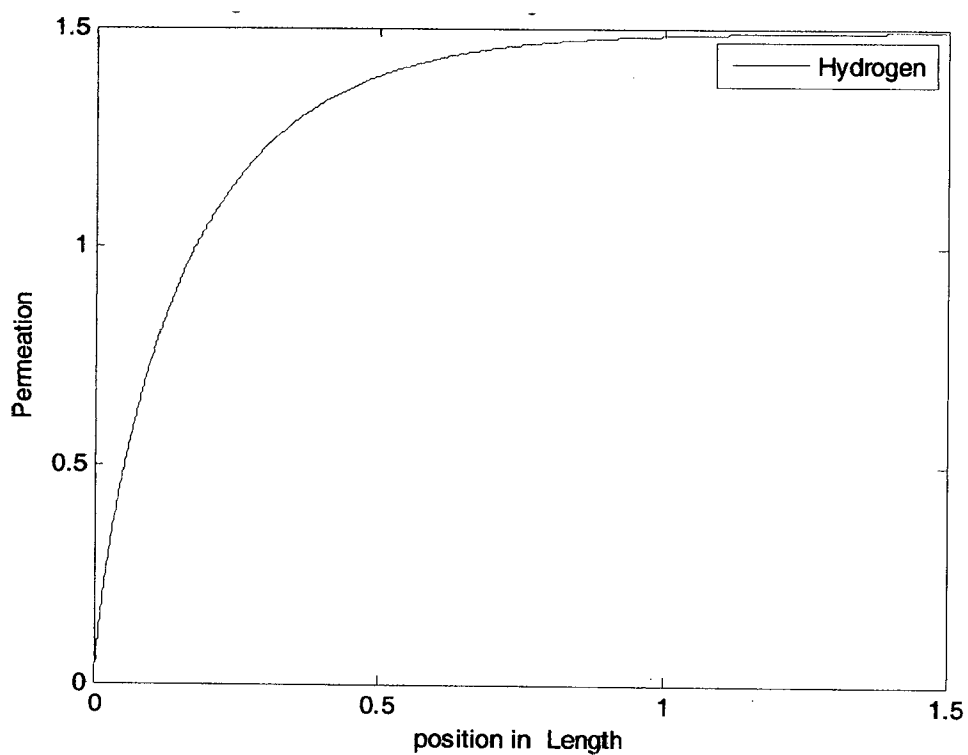


Fig: 34 Effect of Reactor length on H₂ recovery yield in PFR model at 773 K

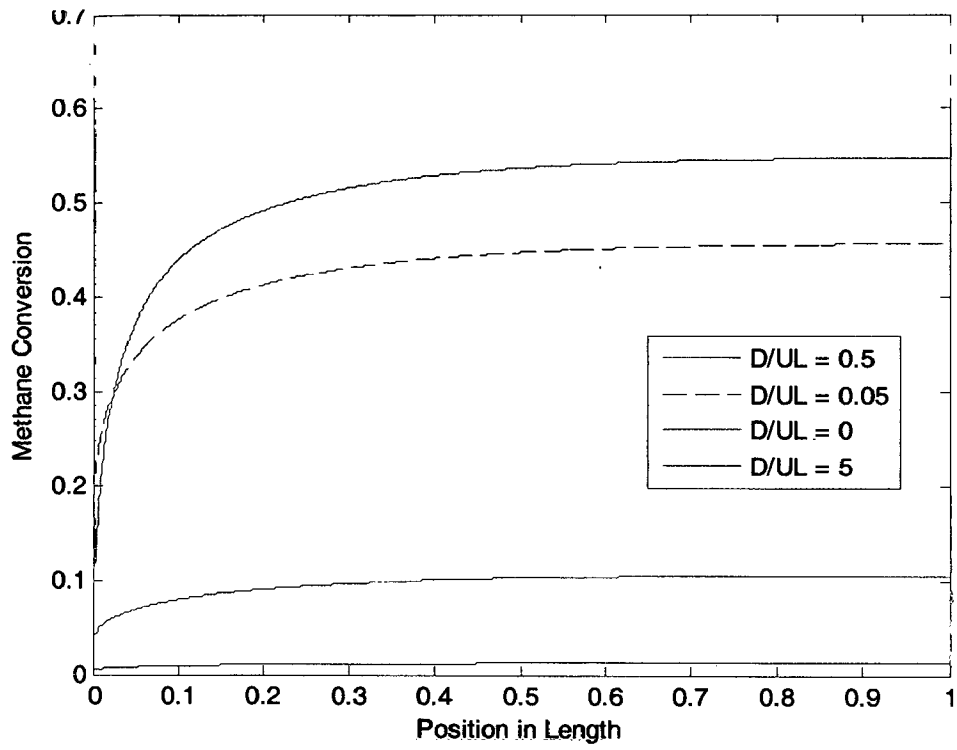


Fig: 35 Effect of reactor length on CH_4 conversion in axial dispersion model 773 K

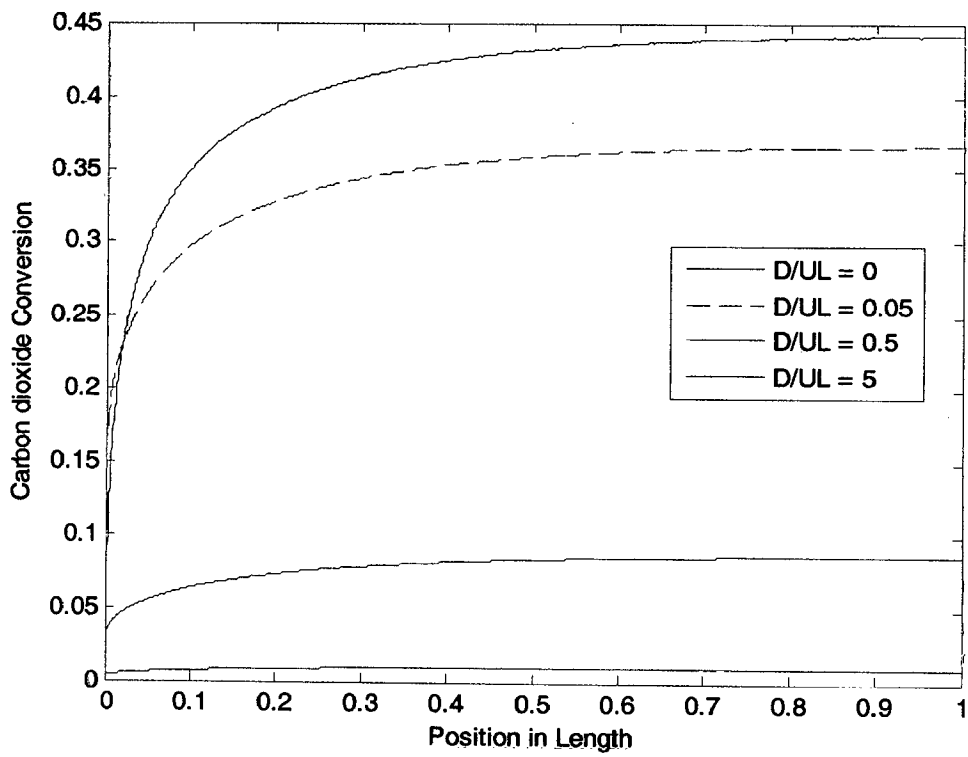


Fig: 36 Effect of reactor length on CO_2 conversion in axial dispersion model 773 K

CONCLUSIONS AND RECOMMENDATIONS

In this study the independent eight parameters affecting the conversions of CH_4 , CO_2 and H_2 recovery yield are calculated and presented in the form of graphs. It is shown in every parameter effect, that the non ideal nature will not be good to have more achievable conversions. So care has to be taken in designing operational strategy such that it is nearer to ideal behaviour. Effects of steam to methane ratio and temperature have to be kept in consideration while designing operational strategy. Further in this study, pseudo homogeneous model is assumed by which the effect of porosity is not considered. As the reaction is taking place in catalyst surface, porosity effect can not be neglected. So it is recommended to consider porosity effect in the future work. Here, in this work dispersion coefficient is taken as constant but it itself is a dependent parameter on physical parameters of the experiment. For example Knudsen diffusion coefficient is depends on average velocity and diameter of particle. So effect of various parameters on axial dispersion coefficient can not be neglected. It is also recommended to conduct the experiment and study the results through back-flow cell model.

BIBLIOGRAPHY:

1. Assaf. E.M, C.D.F.Jesus and J. M. Assaf, "Mathematical modeling of methane steam reforming in a membrane reactor: an isothermal model", *Brazilian journal of chemical engineering, free e-journal*, 15, no. 2, São Paulo, June 1998.
2. Fabiano A.N. Fernandez, Aldo B. Soares Jr "Methane steam reforming modeling in a palladium membrane reactor", *Fuel*, 85, (2006), pp 569–573
3. Fausto gallucci, Antonio comite, Gustavo capannelli, and Angelo basile, "Steam reforming of methane in a membrane reactor: an industrial case study", *Ind. Eng. Chem. Res.* 45, (2006), pp 2994-3000
4. Fausto gallucci, Luca paturzo, Angelo fama, and Angelo basile "Experimental study of the methane steam reforming reaction in a dense Pd/Ag membrane reactor", *Ind. Eng. Chem. Res.* 43, (2004), pp 928-933.
5. Giuseppe barbieri, Giuseppe marigliano, Giovanni perri, and Enrico drioli "Conversion temperature diagram for a palladium membrane reactor. Analysis of an endothermic reaction: methane steam reforming", *Ind. Eng. Chem. Res.*, 40, (2001), pp 2017-2026.
6. Giuseppe barbieri, Vittorio violante, Francesco P. di maio, Alessandra criscuoli, and Enrico drioli "Methane steam reforming analysis in a palladium-based catalytic membrane reactor", *Ind. Eng. Chem. Res.*, 36 (1997), pp 3369-3374
7. Hacarlioglu .P, Y. Gu, s. T. Oyama "Studies of the methane steam reforming reaction at high pressure in a ceramic membrane reactor", *Journal of Natural Gas Chemistry*, 15, (2006), pp 73-81
8. Jianhua tong and Yasuyuki matsumura "Effect of catalytic activity on methane steam reforming in hydrogen-permeable membrane reactor", *Applied catalysis A: general*, vol 286, issue 2, (2005), pp 226-231.
9. Jun shu, Bernard P.A. Grandjean, Serge kaliaguine "Methane steam reforming in asymmetric Pd and Pd-Ag/SS membrane reactors", *Applied catalysis A: General*, 119, (1994), pp 305-325.
10. Kim aasberg-petersen, Charlotte stub Nielsen, Susanne Laegsgaard jørgensen "Membrane reforming for hydrogen", *Catalysis today*, 46, (1998), pp 193-201.
11. Laegsgaard jørgensen .S, P.E.Højlund Nielsen, P. Lehrmann "Steam reforming of methane in membrane reactor", *Catalysis Today*, 25, (1995), pp 303-307.
12. Lin Y.M, Shu ling liu, Chenhsien chuang, Yao tung chu "Effect of incipient removal of hydrogen through palladium membrane on the conversion of methane steam reforming experimental and modeling", *Catalysis Today*, 82, (2003), pp 127–139.

13. Luca paturzo and Angelo basile “Methane conversion to syngas in a composite palladium membrane reactor with increasing number of pd layers”, *Ind. Eng. Chem. Res.* 41, (2002), 1703-1710
14. Oklany J. S, k. Hou and R. Hughes “A simulative comparison of dense and micro porous membrane reactors for the steam reforming of methane”, *Applied Catalysis A: General*, vol 170, issue 1, (1998), pp 13-22
15. Paloma ferreira, Aparicio and Manuel J. Benito “High performance membrane reactor system for hydrogen production from methane”, *Ind. Eng. Chem. Res.* 44, (2005), 742-748.
16. Perry’s Chemical Engineering Hand Book. 7th edition, Mc Graw Hill New York , 5-72.
17. Shigeki Haraa, Giuseppe Barbieria, Enrico Driolia “Limit conversion of a palladium membrane reactor using counter-current sweep gas on methane steam reforming”, *Desalination*, 200, (2006), pp 708–709,
18. Shigeyuki Uemiya, Noboru Sato, Hiroshi ando, Takeshi matsuda, Eiichi kikuchi “Steam reforming of methane in a hydrogen permeable membrane reactor”, *Applied catalysis*, 67, (1991), pp 223-230
19. Tiemersma, T.P. C.S. Patil, M. van Sint Annaland J.A.M. Kuipers “Modeling of packed bed membrane reactors for auto thermal production of ultra pure hydrogen”, *Chemical Engineering Science*, 61, (2006), pp 1602 – 1616.
20. Tsoitsis .T.T, A.M.Champagnie, S.P.Vasileiadis, R.G.Minet “Packed bed catalytic membrane reactors”, *Chemical Engineering Science*, 47, (1992), pp 2903-2908.
21. Xu J, Froment.G.F “Methane steam reforming, methanation and water gas shift: intrinsic kinetics”, *AICHE Journal*, 35, (1989), pp 88-96.

5. APPENDIX

1. MATLAB Model to solve PFR model equations and comparing them with literature.

```
function [z,x]=solvemod(l)
zspan=[0 l];
x0=[0;0;0];
[z,x]=ode45(@steamrefmod,zspan,x0,l);
```

```
function dxdz=steamrefmod(z,x)
```

%Factors Used	%Description	Units
m=3;	% H2O/CH4 ratio	No
n=0.0000295;	% $p(H_2,0)/p(H_2)=p_{61}/p_6$	No
pr=136000;	% reaction pressure	Pa
pp=100000;	% permeation pressure	Pa
tr=773;	% Reaction temperature Kelvin	K
I=42/42;	% sweep factor	No
Do=0.017;	% Outer tube's inner dia	M
Di=0.0095;	% Inner tube's outer dia	M
wt=11/1000;	% weight of catalyst	Kg
vol=pi*(Do ² -Di ²)*l/4;	% volume of reaction zone	Meter Cube
roe=wt/vol;	% Catalyst density	Kg/(Meter Cube)
FA0=42/(16*6*1.4*10000);	% CH4 flow rate	mol/s
thk=20*(10 ⁻⁶);	% Membrane thickness	M
Ru=8.314;	% Universal gas constant	J/(mol.K)

% 4=CH4; 5=H2O; (6=H2; 61=H2,0; 62=H2,p; 63=H2,array); 7=CO; 8=CO2

%Pre exponential factors	Description	Units
k10=(3.7112842e+017);	%Rate coefficient of Reaction 1	mol.(pa ^{0.5})/(kg cat.S)
k20=5.43055556;	% Rate coefficient of Reaction 2	mol/(Kg cat.Pa.S)
k30=(8.95978670e+016);	% Rate coefficient of Reaction 3	mol.(pa ^{0.5})/(kg cat.S)
K10=(5.75e+022);	% Equilibrium constant for Reaction 1	Pa ²
K20=(1.26/100);	% Equilibrium constant for Reaction 2	No
K30=(7.24e+020);	% Equilibrium constant for Reaction 3	Pa ²
K40=(6.65e-009);	% Adsorption constant for CH4	1/pa

K50=177000;	% Dissociative adsorption constant of H2O	No
K60=(6.12e-014);	% Adsorption constant for H2	1/Pa
K70=(8.23e-010);	% Adsorption constant for CO	1/Pa
Q0=6.96428571e-007;	% Permeation flux	mol/(M.S.Pa^0.5)

	%Description	Units
E11=240.1*1000;	% Reaction1	J/mol
E12=67.13*1000;	% Reaction2	J/mol
E13=243.9*1000;	% Reaction3	J/mol
E21=11476*Ru;	% Equilibrium1	J/mol
E22=-4639*Ru;	% Equilibrium2	J/mol
E23=21646*Ru;	% Equilibrium3	J/mol
E4=-38.28*1000;	% Adsorption activation Energy of CH4	J/mol
E5=88.68*1000;	% Adsorption activation Energy of H2O	J/mol
E6=-82.9*1000;	% Adsorption activation Energy of H2	J/mol
E7=-70.65*1000;	% Adsorption activation Energy of CO	J/mol
Ep=15700;	% coefficient of permeation flux	J/mol

k1=k10*exp(-E11/(Ru*tr));

k2=k20*exp(-E12/(Ru*tr));

k3=k30*exp(-E13/(Ru*tr));

K1=K10*exp(-E21/(Ru*tr));

K2=K20*exp(-E22/(Ru*tr));

K3=K30*exp(-E23/(Ru*tr));

K4=K40*exp(-E4/(Ru*tr));

K5=K50*exp(-E5/(Ru*tr));

K6=K60*exp(-E6/(Ru*tr));

K7=K70*exp(-E7/(Ru*tr));

Q=Q0*exp(-Ep/(Ru*tr));

p63=roots([n (1+m+2*x(1)-x(3))-n*pr) -pr*(3*x(1)+x(2)-x(3))]);

if(p63(2,:)>p63(1,:))

 p6=p63(2,:);

else

```

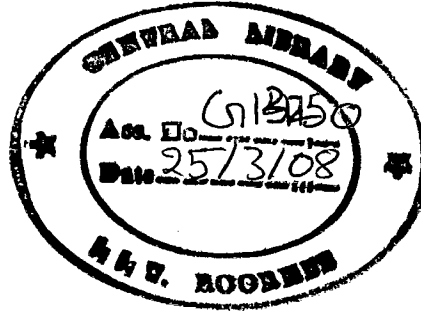
p6=p63(1,:);
end

a=(1+m+n*p6+2*x(1)-x(3))/pr;
p4=(1-x(1))/a;
p5=(m-x(1)-x(2))/a;
p62=pp*x(3)/(x(3)+I);
p7=(x(1)-x(2))/a;
p8=x(2)/a;
D=1+K7*p7+K6*p6+K4*p4+K5*p5/p6;

R1=k1*(p4*p5-(p6*p6*p6*p7/K1))/(D*D*(p6^2.5));
R2=k2*(p7*p5-(p6*p8/K2))/(D*D*p6);
R3=k3*(p4*p5*p5-(p6*p6*p6*p6*p8/K3))/(D*D*(p6^3.5));

dxdz=[pi*(Do^2-Di^2)*roe*(R1+R3)/(4*FA0);
      pi*(Do^2-Di^2)*roe*(R3+R2)/(4*FA0);
      pi*Di*Q*(sqrt(p6)-sqrt(p62))/(thk*FA0)];
end
subplot(3,1,1);plot(z,x(:,1));xlabel('Length (M)');ylabel('Conversion (X CH4)');%gttext('X
CH4');
subplot(3,1,2);plot(z,x(:,2));xlabel('Length (M)');ylabel('Conversion (X CO2)');%gttext('X
CO2');
subplot(3,1,3);plot(z,x(:,3));xlabel('Length (M)');ylabel('Permeation (Y H2)');%gttext('Y H2');
end

```



13250

2. MATLAB Model to solve axial dispersion model equations and comparing them with PFR

model

```
function [u,w,y]=impdispersion(dc)
[z1,f]=ode45(@steamrefmod,[0 1],[0;0;0]);
N=length(z1);
AA=zeros(N-1,N-1);
u=zeros(1,N-1);u1=zeros(1,N);u1(1)=0;
w=zeros(1,N-1);w1=zeros(1,N);w1(1)=0;
y=zeros(1,N-1);
lt1=zeros(N-1);lt2=zeros(N-1);
for i=1:N
    u(i)=f(i,1);
    w(i)=f(i,2);
    y(i)=f(i,3);
end
l=z1(2)-z1(1);
AA(1,1)=-((2*dc/(l*1))-(1/l));
AA(1,2)=((dc/(l*1))-(1/l));
for i=2:N-2
    l=z1(i)-z1(i-1);
    AA(i,i-1)=dc/(l*1);
    AA(i,i)=-((2*dc/(l*1))-(1/l));
    AA(i,i+1)=((dc/(l*1))-(1/l));
end
AA(N-1,N-2)=1;
AA(N-1,N-1)=-1;
for i=1:N-2
    dxdz=steamrefmod(z1(i),[u(i),w(i),y(i)]);
    lt1(i)=-dxdz(1);
    lt2(i)=-dxdz(2);
end
lt1(N-1)=0;
lt2(N-1)=0;
```

```

u=AA\lt1;
w=AA\lt2;
for i=2:N
    u1(i)=u(i-1);
    w1(i)=w(i-1);
end
function dxdz=steamrefmod(z,x)
    %Factors Used    % Description          Units
    m=3;            % H2O/CH4 ratio        No
    L=0.036;        % Reactor Length      M
    n=0.0000296;    % p(H2,0)/p(H2)       No
    pr=136000;      % reaction pressure    Pa
    pp=100000;      % permeation pressure  Pa
    tr=773;         % Reaction temperature Kelvin K
    I=42/42;        % sweep factor         No
    Di=0.0095;      % Inner tube's outer dia, M
    wt=11/1000;     % weight of catalyst   Kg
    FA0=42/(16*6*1.4*10000); % CH4 flowrate        mol/s
    thk=20*(10^-6); % Membrane thickness   M
    Ru=8.314;       % Universal gas constant J/(mol.K)
    % 4=CH4; 5=H2O; 6=H2; 62=H2,p; 7=CO; 8=CO2

```

```

%Pre exponential factors    Description          Units
k10=(3.711284198392056e+017); % Rate coefficient of Reaction 1 mol.(pa^0.5)/(kg cat.S)
k20=5.430555555555556;      % Rate coefficient of Reaction 2 mol/(Kg cat.Pa.S)
k30=(8.95978670e+016);      % Rate coefficient of Reaction 3 mol.(pa^0.5)/(kg cat.S)
K10=(5.75e+022);            % Equilibrium constant for Reaction 1 Pa^2
K20=(1.26/100);             % Equilibrium constant for Reaction 2 No
K30=(7.24e+020);            % Equilibrium constant for Reaction 3 Pa^2
K40=(6.65e-009);           % Adsorption constant for CH4 1/pa
K50=177000;                 % Dissociative adsorption constant of H2O No
K60=(6.12e-014);           % Adsorption constant for H2 1/Pa
K70=(8.23e-010);           % Adsorption constant for CO 1/Pa
Q0=6.964285714285715e-007; % Permeation flux mol/(M.S.Pa^0.5)

```

	%Description	Units
E11=240.1*1000;	% Reaction1	J/mol
E12=67.13*1000;	% Reaction2	J/mol
E13=243.9*1000;	% Reaction3	J/mol
E21=11476*Ru;	% Equilibrium1	J/mol
E22=-4639*Ru;	% Equilibrium2	J/mol
E23=21646*Ru;	% Equilibrium3	J/mol
E4=-38.28*1000;	% Adsorption activation Energy of CH4	J/mol
E5=88.68*1000;	% Adsorption activation Energy of H2O	J/mol
E6=-82.9*1000;	% Adsorption activation Energy of H2	J/mol
E7=-70.65*1000;	% Adsorption activation Energy of CO	J/mol
Ep=15700;	% permeation flux constant	J/mol
k1=k10*exp(-E11/(Ru*tr));		
k2=k20*exp(-E12/(Ru*tr));		
k3=k30*exp(-E13/(Ru*tr));		
K1=K10*exp(-E21/(Ru*tr));		
K2=K20*exp(-E22/(Ru*tr));		
K3=K30*exp(-E23/(Ru*tr));		
K4=K40*exp(-E4/(Ru*tr));		
K5=K50*exp(-E5/(Ru*tr));		
K6=K60*exp(-E6/(Ru*tr));		
K7=K70*exp(-E7/(Ru*tr));		
Q=Q0*exp(-Ep/(Ru*tr));		
B=pi*Di*Q*L/(thk*FA0);		
b1=(1+m+2*x(1)-x(3)-n*pr);		
c1=-pr*(3*x(1)+x(2)-x(3));		
p6=(-b1+sqrt(b1*b1-4*n*c1))/(2*n);		
a=(1+m+n*p6+2*x(1)-x(3))/pr;		
p4=(1-x(1))/a;		
p5=(m-x(1)-x(2))/a;		
p62=pp*x(3)/(x(3)+1);		
p7=(x(1)-x(2))/a;		
p8=x(2)/a;		

```

D=1+K7*p7+K6*p6+K4*p4+K5*p5/p6;

R1=k1*(p4*p5-(p6*p6*p6*p7/K1))/(D*D*(p6^2.5));
R2=k2*(p7*p5-(p6*p8/K2))/(D*D*p6);
R3=k3*(p4*p5*p5-(p6*p6*p6*p6*p8/K3))/(D*D*(p6^3.5));

dxdz=[wt*(R1+R3)/FA0;
      wt*(R2+R3)/FA0;
      B*(sqrt(p6)-sqrt(p62))];
end
subplot(3,2,1);plot(z1,u1);xlabel('Length (M)');ylabel('Conversion (X CH4)');title('Dispersive
flow model');
subplot(3,2,2);plot(z1,w1);xlabel('Length (M)');ylabel('Conversion (X CO2)');title('Dispersive
flow model');
subplot(3,2,3);plot(z1,y);xlabel('Length (M)');ylabel('Permeation (Y H2)');title('Dispersive flow
model');
subplot(3,2,4);plot(z1,f(:,1));xlabel('Length (M)');ylabel('Conversion (X CH4)');title('PFR
model');
subplot(3,2,5);plot(z1,f(:,2));xlabel('Length (M)');ylabel('Conversion (X CO2)');title('PFR
model');
subplot(3,2,6);plot(z1,f(:,3));xlabel('Length (M)');ylabel('Permeation (Y H2)');title('PFR
model');
end

```